Physical and biological influences on daily growth rate of larval alewife (*Alosa pseudoharengus*) in Lake Michigan

by
Sara Prendergast

A thesis submitted
in partial fulfillment of the requirements
for the degree of Master of Science
(Environment and Sustainability)
at the University of Michigan
2019

Thesis Committee:
      Dr. Karen Alofs, Chair
      Dr. Mark Rowe
      Dr. Edward Rutherford

Abstract

Alewife is an invasive fish species in the Great Lakes that serves as prey for top piscivores but also causes reproductive failure of some native species. Environmental conditions generating variability in annual abundance of young alewife are poorly known, but are hypothesized to occur during the sensitive larval stage through advection of larvae into, or away from areas that support rapid larval growth. We modeled transport of alewife larvae from capture to hatch locations, and tested the hypothesis that daily growth of larval alewife can be predicted from environmental conditions. We analyzed growth rates of larval alewife that were sampled from multiple sites in Lake Michigan in July 2015, and estimated their ages and daily growth rates by counting and measuring daily increment widths of their otoliths. We used a Lagrangian particle dispersion model to conduct a backwards trajectory analysis of known-aged larvae from their capture locations to their hatch locations. The trajectory results indicated that larvae collected from sites in western and eastern Lake Michigan hatched at locations along the eastern shoreline. We paired trajectory paths with environmental conditions predicted from a biophysical model. We used a mixed model and found a significant positive relationship between larval daily growth rate and temperature, detritus, and zooplankton concentrations. These results suggest areas and environmental conditions that are favorable to young alewife growth in Lake Michigan.

Acknowledgements

Table of Contents

Introduction

The connection between transport of larval fish and recruitment variability has long been recognized (Hjort 1914), and this link underlies the importance of understanding the different environments larval fish encounter during their planktonic stage. Physical processes can control recruitment by altering the biological and physiochemical environments larval fish experience (Ludsin et al. 2014). Growth and mortality rates of larval fish are important to recruitment success (Houde 1987), but the mechanisms underlying these processes (e.g., temperature, prey availability, predation, water circulation) are not always clear (Pritt et al. 2014). Multiple hypotheses attempt to explain mechanisms behind recruitment variability in fishes. In the critical period hypothesis, variation in year class strength is determined in the first year of life as currents push larvae into or away from favorable nursery habitats (Hjort 1914). Cushing's match-mismatch hypothesis suggests that variability in fish year class strength is linked to variability in timing of plankton production with larval occurrence (Cushing 1990). These hypotheses and several other influential recruitment hypotheses (e.g., stable-ocean (Lasker 1978); optimal window (Cury and Roy 1989)) were developed from studying the marine environment, but do not always hold true in freshwater habitats (Pritt et al. 2014).

There are clear differences between physical processes in marine systems and those in large freshwater systems that may affect fish larvae growth, survival and potential recruitment. The Great Lakes are enclosed systems compared to most marine habitats, and their smaller size causes higher spatial and temporal variability in physical processes than most marine systems (Pritt et al. 2014). Large-scale circulation patterns in the Great Lakes are primarily wind driven. Long-term currents are weak compared to the stronger and more unpredictable wind-induced short-term currents (Beletsky et al. 1999). Circulation in the nearshore zone, an area from the shoreline to 20-m bathymetric depth, is influenced by topographic boundaries of the shorelines with coastal flow largely parallel to the shorelines (Rao and Schwab 2007). Due to the nature of the Coriolis force in the northern hemisphere, Ekman transport moves surface currents to the right of the wind stress. This results in coastal upwelling and downwelling in which the thermocline is either raised or lowered in the water column within the coastal boundary layer, a region between the open lake and the wave breaking zone that is 5 to 10-km wide (Rao and Murthy 2001). When the lakes are stratified, currents often exhibit inertial oscillations which are the result of the Coriolis force that deflects the path of a moving object to the right, creating a circular trajectory. In Lake Michigan, the inertial period is between 17 and 18 hours (Mortimer 2006) and is altered by wind stress. Inertial oscillations occur in the offshore region, and as they move into the coastal boundary layer they are modified by their diminishing velocities (Rao and Schwab 2007). The physical processes within the coastal boundary layer include these modified inertial oscillations, coastal transport, and upwelling/downwelling events. Many organisms spawn and hatch in the nearshore zone and are influenced by the physical processes of both the nearshore zone and coastal boundary layer.

Fish recruitment, as it relates to physical and biological coupling, has largely been studied in the marine environment. In the past two decades, efforts to understand recruitment have increased in freshwater ecosystems such as the Great Lakes (Ludsin et al. 2014). This

comes at an important time when the ecosystems of the Great Lakes are changing with the introduction of dreissenid mussels and the resultant decline in pelagic primary production (Rowe et al. 2015b) and prey fish populations (Bunnell et al. 2014).

Alewife (*Alosa psuedoharengus*) is an economically important prey fish of Lake Michigan. Initially an unwelcome invasive species to the Great Lakes, alewife became the primary food source for stocked Pacific salmonids that has resulted in a multi-billion dollar fishery. Due to the tightly-coupled predator-prey interactions between salmonids and alewife within the Great Lakes, maintaining stable populations of alewife success is a keen management interest. In recent years, alewife biomass has declined in Lake Michigan (Madenjian et al. 2017), and there is growing concern that the population will collapse as it did in Lake Huron in 2003 (Riley et al. 2008; Dunlop and Riley 2013). In Lake Huron, predation pressure from salmonids and lack of food availability from competition with the invasive Dreissenid mussels led to the collapse of alewife (Kao et al. 2016). Shortly after, salmonid populations collapsed (Johnson et al. 2010) with no signs of recovery (Clark et al. 2017). To protect Lake Michigan against a similar outcome, there is interest in maintaining the alewife population at a level that can support predator demands and still be supported by lower trophic levels (Eggold et al. 2018).

Environmental conditions vary both spatially and temporally throughout Lake Michigan (Beletsky et al. 2007; Rowe et al. 2017). Due to the large latitudinal range of the lake, there is a strong north-south thermal gradient. The southern basin is shallower than the northern basin, warms earlier, and has large changes in wind-induced circulation when compared with the northern basin (Beletsky et al. 2006). Winds are predominately from the west or southwest and are associated with upwelling on the western side and downwelling on the eastern side of the lake. Upwelling brings cooler, dense, nutrient rich waters to the surface while downwelling depresses the thermocline and is associated with warm surface waters. There are also seasonal differences with stratification increasing throughout the summer months and wind-induced mixing causing isothermal conditions during winter months. The currents in Lake Michigan vary between the nearshore and offshore environment and control the transport of planktonic larvae (Rao and Schwab 2007; Beletsky et al. 2017).

The large-scale environmental differences in Lake Michigan make models valuable tools for estimating physical transport and environmental conditions. Several studies have used models to assess the impact of water currents on the distribution of planktonic yellow perch (*Perca flavescens*) and found potential for the currents to move the larvae over large distances (Beletsky et al. 2004; Dettmers et al. 2005; Brodnik et al. 2015). Beletsky et al. (2007) used a hydrodynamic model and an individual-based bioenergetics model to track yellow perch hatching in the southern basin of Lake Michigan and found that larval fish could move as far as the northern basin (approximately 320 km) with a drifting stage lasting between 63 and 77 days. They were also able to predict water temperatures but assumed uniform zooplankton abundance due to limited spatial data. This type of analysis provides insight into fish recruitment dynamics, but is limited by the accuracy of the models and available data. Improving on the work of Beletsky et al. (2007), Rowe et al. (2017) coupled a hydrodynamic model specific to Lake Michigan with a phosphorous-limited lower food web model to predict spatially and temporally varying phytoplankton and zooplankton abundance. Since then, further improvements have

been made for the hydrodynamic models of the Great Lakes and the Lake Michigan-Huron Operational Forecasting System (LMHOFS) has been developed. This model is based on the Finite Volume Community Ocean Model (FVCOM), and compared with previous hydrodynamic models of Lake Michigan, has a higher spatial resolution in nearshore areas (~0.5 km) and a more accurate representation of the coastal morphology as a result of the unstructured grid of the FVCOM (Anderson and Schwab 2013).

A backward-trajectory analysis can be applied to predict drift trajectories of larval fish or other constituents that are carried by currents based on their ending location (Brodnik et al. 2015). For larval fish, age data can be obtained from the otoliths (ear bones) and can be applied to a Lagrangian particle dispersion model to estimate the trajectory of a larvae for the duration of its life from the location of capture back to the hatch location (Brodnik et al. 2015). Several studies have assessed the impact of currents on connectivity of fish populations using a backward trajectory analysis (Brodnik et al. 2015; Caló et al. 2018).

A Previous study of larval alewife in Lake Michigan addressed the role of environment on growth rate of larval alewife (Eppeheimer et al. 2019). The study analyzed environmental characteristic from capture sites to assess growth rate, but did not assess the role of transport on larval growth rate and survival. My objective was to address the role of physical transport and environmental conditions on larval alewife growth rate. I assessed the accuracy of modeled backwards trajectories using observed trajectories from satellite-tracked drifting buoys. I estimated the age and daily growth rate of larval alewife using otolith increment analysis. By combining age with the Lagrangian particle dispersion model and estimates of temperature and food availability from the biophysical model, I approximated the environmental conditions experienced by larval alewife on each day of their life from hatch to the time of capture. I also estimated the hatch location of larvae collected from around Lake Michigan. Finally, I used a statistical model to evaluate the impact of environmental conditions on daily growth rate. I hypothesized that the daily growth rate of larval alewife can be predicted from their exposure to environmental conditions (temperature, zooplankton concentrations, phytoplankton concentrations, detritus concentrations) from hatch to capture. My goal is to enhance understanding of factors generating variability in fish year-class strength and recruitment success.

Methods

Larval Alewife Collections

Larval alewife samples were collected between July 8-27, 2015 in Lake Michigan by the United States Geological Survey (USGS) Great Lakes Science Center (GLSC) as part of the multi-agency Cooperative Science and Monitoring Initiative (CSMI). Collections were made along six transects offshore of Ludington, MI; Saugatuck, MI; St. Joseph, MI; Waukegan, IL; Racine, WI; and Manitowoc, WI (Figure 1). Three bathymetric depth sites (18-m, 46-m, and 91 or 110-m) were sampled along each transect. Both a surface ichthyoplankton (IP) tow and an oblique IP tow were performed at each site and all sampling was completed at night when alewife larvae move higher into the water column (Madenjian and Jude 1985). Further details of the collection methods are outlined by Eppehimer et al. (2019). A temperature profile of each sampling site

was collected using a bathythermograph (SBE19plus; Sea-Bird Scientific, Bellevue, WA). Larval alewife were present and collected at all sites with the exception of Manitowoc, WI (only collected at 110-m) and Ludington, MI (only collected at 46-m and 110-m) (Figure 1).

Alewife Otolith Analysis

I used sagittal otoliths to estimate age and measure growth increments of larval alewife as these are considered to be the most precise structure for this type of analysis (LaBay and Lauer 2006). Daily otolith growth increments have been previously used as a proxy for alewife age (Höök et al. 2007; Eppehimer et al. 2019). The first ring is likely laid on the second day of life (Essig and Cole 1986); thus, I added two to the number of increments counted to determine the age of the larval fish. I took images of the otoliths using an imaging system (QICAM 12-bit; Teledyne QImaging, Surrey, BC, Canada), and I measured the otolith diameter and increment widths using image analysis software (Image-Pro Premier Version 9.0; Media Cybernetics, Inc., Rockville, Maryland). I quantified daily incremental rings and measured distances between rings measured along the longest and clearest transect from the center of the nucleus to the outer edge of the otolith. I observed otoliths under 1000x magnification (oil-immersed 100x objective lens; with 10x eyepiece lenses).

I used a rigorous method when estimating ages of larval alewife to ensure minimal disparity between age estimates by different analysts. Previous age estimates of the samples were performed by Eppehimer et al. (2019) where two analysts individually read each otolith. If the difference between the readings was less than 10% the average was taken. If the difference was greater than 10%, the two analysts conducted a second reading. If there was still disagreement, a third analyst performed an independent reading and the median of the final three readings was used. I conducted my own age estimates and compared them to those of Eppehimer et al. (2019). If my age estimate differed by more than one day from the previously estimated age by Eppehimer et al. (2019), a second analyst counted the rings, and if the estimate from the second analyst differed by more than a day from the reading by Eppehimer et al. (2019), the sample was omitted from the study. If the second analyst was within a day from the estimate by Eppehimer et al. (2019), the first and second analyst tried to come to an agreement about the age, and if no agreement could be made, the sample was omitted from the study. In total, I aged 290 alewife larvae that were included in analyses. To ensure that sampled larvae were passive drifters, I excluded fish larger than 22 mm total length (TL) because the alewife larval stage lasts between 30-40 days and alewife ≤ 22 mm are most likely larvae (Klumb et al. 2003; Norden 1967).

Satellite Tracked Drifting Buoys

Satellite drifters were deployed and tracked offshore of Muskegon, MI on three separate occasions in 2018. The University of Maryland deployed satellite tracked drifting buoys offshore of Muskegon, MI in 2015 (Figures 2, 3). In 2018, three drifters were released at M15, M45, and M110 on the first deployment starting June 5, 2018 and retrieved June 12, 2018. Site names represent bathymetric contours at 15-m, 45-m, and 110-m, respectively. In the second deployment, another three drifters were released on June 27, 2018, with one released at M15

and two released 12 hours apart at M45. All drifters washed up on the beach by July 4, 2018. For the third deployment, three more drifters were released on July 18, 2018 at M15, M45, and, M110, and were retrieved on shore August 5, 2018. All release dates were during periods when alewife were present and passively drifting in the water column (Heufelder et al. 1982). In 2015, The University of Maryland/NOAA deployed drifters off Muskegon, MI starting June 30, 2015. Three of the six deployed drifters drifted for approximately one month, and I used results of those three drifters in this study (Figure 3) (https://www.nefsc.noaa.gov/drifter/drift_umaryland_2015_1.csv). All drifters extend approximately 1-m below the water's surface and track surface currents. They are designed after the "Eddie" drifter described by NOAA's Northeast Fishery Science Center (https://www.nefsc.noaa.gov/epd/ocean/MainPage/lob/driftdesign.html), with a cruciform drogue with floats attached to the center column. An attached Global Positioning System (GPS) transmitter (SmartoneBLP; Globalstar, Chantilly, Virginia) at the top of the platform estimated drifter position hourly in 2018 and every two hours in 2015. I calculated current speeds in Lake Michigan in 2015 and 2018 using data from drifter deployments. Distance between positional output was calculated and estimated as a water velocity (m s^{-1}).

Hydrodynamic and biophysical models

The Lake Michigan-Huron Operational Forecast System (LMHOFS) model is a hydrodynamic model implemented by NOAA for real-time nowcast and forecast predictions of water levels, currents, and temperatures (Anderson and Schwab, 2013; 2017), and became a NOAA operational model in July, 2019 (https://tidesandcurrents.noaa.gov/ofs/dev/lmhofs/lmhofs.html). The LMHOFS model is an application of the Finite Volume Community Ocean Model (FVCOM); a three-dimensional oceanographic model that implements a numerical solution of the momentum, continuity, temperature, salinity, and density equations (Chen et al. 2006; http://fvcom.smast.umassd.edu/). FVCOM has been applied to the Great Lakes with successful simulations of current velocity and direction, seasonal stratification, and temperature profiles (Anderson and Schwab 2013; Bai et al. 2013). I used hydrodynamic output from the LMHOFS model for 2015 and 2018 using meteorological forcing from the high-resolution rapid refresh (HRRR) model (Benjamin et al. 2016) to model drifter runs and larval fish trajectories backwards through time. The vertical dimension is defined using terrain following (sigma) coordinates with 20 sigma layers.

The Lagrangian particle tracking model (Huret et al. 2007; Churchill et al. 2011; Rowe et al. 2016) is distributed as part of the FVCOM code package (http://fvcom.smast.umassd.edu/). I used the Lagrangian particle tracking model forced with currents and diffusivity from the LMHOFS model to simulate the movement of larval fish and drifters. A fixed time step of 600 s was used with a fourth-order Runge-Kutta scheme (Rowe et al. 2016). To limit the effects of random noise in the simulation, I initiated simulations with 1000 particles (Rowe et al. 2016) placed in the surface layer. A vertical velocity component used to represent floating/sinking/swimming was implemented. I ran simulations with both horizontal and vertical random walk to capture the combined effects of sub-grid-scale fluid motions in the nature of turbulent flow within the system. I applied a backwards-trajectory to the model, initiating the particles at the

capture location and running the model for a length of time representing the age of the fish. The end location is the estimated hatch location of the larvae.

I defined the nearshore environment, where alewife spawn, as the region between the shoreline out to the 20-m bathymetric contour (Withers et al. 2015). I divided Lake Michigan into a 90 x 90 grid (~1.6 km X 1.6 km) and calculated probability of predicted hatch location by summing particle end locations in each grid space and dividing by the total number of particles. A probability was calculated only for trajectories that indicated potential hatch locations for larval fish in the nearshore environment. I used a nearest neighbor interpolation to smooth the probability raster over a 3 x 3 grid cell area to better represent low probability areas. I calculated the centroid of the particle patch and measured the distance from the centroid to the drifter start location to quantitatively assess model predictions.

I paired backwards trajectories of modeled drifter tracks with drifter observations to calibrate values of horizontal diffusivity (K_H) and vertical velocity for the larval fish simulation. I used all 12 drifter trajectories from both the 2015 and 2018 releases and varied model parameters while taking note of predicted versus observed drifter release locations for transport scenarios representing offshore vs. nearshore drifter releases and alongshore vs. inertial oscillation trajectories. Horizontal diffusion has been studied in the Great Lakes and oceans and is influential in the dispersal of drifting objects. Horizontal diffusivity values in the ocean vary on a length scale of 100-m to 1-km, representative of the FVCOM model grid horizontal resolution, and can range from 1-10 $m^2 s^{-1}$ (Okubo 1971). Compared with oceans, lakes have less wave energy and lack tides, making them potentially less dispersive than oceans. In a diffusion study of the nearshore environment of southern Lake Michigan, Thupaki et al. (2013) estimated the mean horizontal diffusivity value to be 5.6 $m^2 s^{-1}$. Larval fish are weak swimmers, but very low swimming velocities are required to maintain a vertical position in the water column. I assumed larval alewife occurred throughout the epilimnion during the day as there is no evidence that larval alewife exhibit diel vertical migration (Martin et al. 2011). I gave the particles an upward swimming velocity to maintain their position in the epilimnion. I know of no studies in which a vertical swimming velocity has been estimated for alewife larvae, but a study on cod larvae in the Arctic estimated the vertical swimming velocity to be 0.001 m s^{-1} (Vikebo et al. 2007). Using the value of Vikebo et al. (2007) as a benchmark, I calibrated the vertical velocity of alewife to maintain the particles dispersed within the upper 20-m of the water column.

I assessed several transport scenarios using a backwards-trajectory analysis to observe how well the model simulates weak wind forcing (inertial oscillations) and strong wind forcing (coastal boundary currents). I used wind data collected by NOAA/National Buoy Data Center (NBDC) buoy 45161 located off Muskegon, MI for analysis of transport scenarios, using a period from 24 hours prior to drifter release to the end of the drifter track. I used segments of longer drifter runs that exhibited transport scenarios of interest including inertial oscillations, inertial oscillations with a directional shift, and coastal transport.

The biophysical model is a nutrient-phytoplankton-zooplankton-detritus (NPZD) model that simulates dynamics of a phosphorous-limited lower food web. The model includes dissolved phosphorous, phytoplankton, zooplankton, and detritus (nonliving organic matter),

with a fixed carbon-phosphorous stoichiometry. The biophysical model uses the FVCOM general ecosystem model (GEM) to estimate NPZD and temperature by solving advection diffusion equations on the FVCOM unstructured grid (Rowe et al. 2017). FVCOM-GEM was modified to use phytoplankton photosynthesis-irradiance functions measured by Fahnenstiel et al. (1989) and to simulate biomass filtration of phytoplankton by invasive dreissenid mussels (Rowe et al. 2017). Food web parameters were calibrated to reproduce zooplankton biomass observed at a long-term ecological monitoring site offshore of Muskegon (Vanderploeg et al. 2012) in 2000, and assessed against subsequent observations in 2005 and 2010 spanning the period of colonization by invasive quagga mussels (Rowe et al. 2017). The biophysical model was run for 2015 to estimate NPZD concentrations and temperatures throughout Lake Michigan. Meteorology was interpolated from observations. Daily tributary phosphorous loads at 38 locations were estimated using discharge from USGS stream flow gages and the most recent available estimates of annual total and dissolved phosphorous loads (mean of 2006-2008; Dolan and Chapra 2012), as described by Rowe et al. (2017). Dreissenid mussels biomass was initialized from a 2015 lake-wide survey, interpolated using the geostatistical model of Rowe et al. (2015b). Lateral boundaries were closed including the Straits of Mackinac and outflow through the Chicago River (Rowe et al. 2017). I extracted data from output of the biophysical model along trajectories from the Lagrangian particle dispersion model to estimate the NPZD concentrations and temperatures along the modeled trajectories.

Statistical Analysis

I first used a regression tree to explore the relationship between otolith increment width and predictor variables. A regression tree splits the data into smaller subsets by using a process known as binary recursive partitioning. This was done using R.3.6.0 (R core team, 2019), with the r package *rpart.plot* (v3.0.7; Milborrow 2019). I compared two different regression trees, one with all predictor variables (age, temperature, zooplankton, phytoplankton, and detritus) and one without age to visualize the effects variables have on increment width. The regression tree without age allows visualization of other predictor variables on otolith increment width. I calculated the correlation coefficient among the variables and the highest coefficient was among phytoplankton and zooplankton (0.80) and the next highest was between zooplankton and detritus (0.63). The rest of the correlations were below 0.60. I removed phytoplankton from the subsequent mixed model analysis. I performed a linear mixed model analysis to determine the relationship between the estimated environmental conditions (zooplankton, detritus, temperature) and daily increment growth rate of larval fish. Mixed model analysis was completed using the *lmerTest* (v3.1-0; Kuznetsova et al. 2017) and the *interactions* (v1.1-1; Long 2019) packages. A linear mixed model is a regression model that allows for both fixed and random effects. The addition of random effects is necessary when observations are not independent, as with daily otolith increment width of a fish. Individuals and age were included in the mixed model as a random effect. The random effect adds a random intercept and random slope into the model with respect to age, which incorporates the concept that fish grow at different rates as they age into the model. Age was included as an interaction term in the mixed model. I mean centered the variables to predict the effect a single

variable has on the otolith increment while holding all other variables at their mean. Age was not mean centered. Mean centering entails subtracting the mean of the variable from every value of the same variable to redefine the zero point for the predictor variable. Hourly NPZD output was extracted from the biophysical model along backward trajectories predicted by the Lagrangian particle model. Due to computational limitations I had to select a subset of the 1000 particles representing each fish by selecting every 10th particle for a total representation of 100 particles per fish. Otolith increment width was calculated by day, so I averaged NPZD concentrations that each particle experienced over the course of a calendar day before running the mixed model. I checked for the assumption of linearity among the predictor and response variables and normality of the residuals and found that the assumptions held true.

Results

Otolith analysis revealed two important patterns. First, I found an allometric relationship between the total length of alewife larvae and otolith diameter (Figure 4). Second, I found that daily otolith increment width increases with the age of a fish (Figure 5).

I compared observed water velocity from drifters to estimated larval swimming speeds to test the assumption that larval alewife are passive drifters. Swimming at approximately 1-2 body lengths per second, a 22 mm alewife would swim approximately 0.033 m s^{-1} (Klumb et al. 2003). In 2018, between 64.6 and 100% of the time, water velocity calculated from the drifters released on the eastern side of Lake Michigan was faster than the fastest estimated larval swim speeds (Figure S1). In 2015, the water velocity calculated from the drifter deployments on the eastern side of Lake Michigan was faster than estimated larval swim speeds 82% of the time (Figure S2). These results suggest that larval alewife are highly susceptible to current transport in Lake Michigan.

Based upon 2015 and 2018 drifter deployments, I found that drifter transport could be characterized by wind events. Drifters deployed between June 5-12, 2018 exhibited nearshore to offshore transport characterized by inertial oscillations (Figure 2). All three sites (M15, M45, M110) exhibited offshore horizontal transport, but the drifter at M110 moved the furthest horizontally. During that period, the strongest winds were blowing from the north and northwest. A strong north wind causes a wind induced Ekman transport away from the coast along the eastern shore, causing coastal upwelling and offshore transport, as observed in the drifter trajectories. The second drifter deployment on June 27 and 28 was characterized by strong coastal transport. All three drifters moved north along the coast before beaching in the Ludington area on July 4th (Figure 2). The winds were predominately from the south and southeast direction and Ekman transport would be towards the coast, consistent with the observed shoreward and alongshore transport of drifters (Figure 2). South winds are consistent with downwelling events on the eastern shore of Lake Michigan. The third drifter deployment was characterized by initial southward transport exhibiting inertial oscillations followed by northward transport and movement towards shore becoming coastal transport before beaching near Muskegon (Figure 2). The winds were broken down into two separate periods for analysis of that deployment; southward transport and northward transport. Winds during the southward transport were strongest from the north and northwest and were consistent with the southeast

transport of the drifter and upwelling. Winds during the northward transport were more variable, but mostly from the southwest, pushing the drifter towards the shore. In 2015, the drifter trajectories were broken into southward transport and northward transport for wind comparisons. During the southward transport, drifters exhibited transport characteristic of inertial oscillations and winds blew strongly from the north and northwest, consistent with upwelling. When the drifters were moving north, the transport was characteristic of alongshore transport and the winds were from the south (Figure 3). The period during the drifter northward transport is associated with a downwelling event.

Comparisons of Lagrangian particle model backwards trajectories to drifter observations showed that varying horizontal diffusivity (K_H) values influenced the spread of particle dispersal, but did not greatly alter the overall trajectories of particles (Figure 6). The drifter start location was within the spread of the particle patch in all three cases, but the centroid of the particle patch moved closer to the drifter staring location with increasing K_H. Model simulations with varying vertical velocity values showed model particle dispersion is sensitive to vertical velocity. A lower vertical velocity (Figure 7) resulted in more dispersion and greater probability that the initial location is within the particle patch, but the particle depth increased over time. A vertical velocity of 0 m s^{-1} applied to the larval fish resulted in particle depths reaching beyond 100-m, too deep to simulate larval alewife found in the epilimnion. An upwards velocity greater than 0 m s^{-1} was required to keep the particles in the upper 20-m of the water column (Figure 7). A vertical velocity of 0.001 m s^{-1} limited the dispersion of particles both horizontally and vertically (Figure 7). For subsequent simulations, I selected a horizontal diffusivity of 5.6 m^2 s^{-1} and an upward velocity of 0.0003 m s^{-1} to maintain particle vertical position within the upper 20-m of the water column and have a horizontal spread with a greater probability of the backward trajectory particle patch encompassing the initial drifter position.

Modeling all observed drifter tracks from 2015 and 2018 and using the calibrated model, I found that the initial drifter position was within the modeled particle patch 42% of the time (Figure 8). In the segmented 2015 transport scenarios, I found that the initial drifter position was within the modeled particle patch when inertial oscillations were the dominating pattern (Figure 9). Modeled individual particle trajectories demonstrated inertial oscillations similar to observations when winds were predominately from the north and northeast (Figure 9) When there was a wind shift and inertial oscillations were present, the initial drifter position was within the modeled particle patch, but the largest portion of the patch was north of the initial position and individual particle tracks show that the model did not predict the directional shift to the extent observed (Figure 9). When there was strong coastal transport, the initial drifter position was not within the modeled particle patch (Figure 9).

Modeled results of larval fish trajectories revealed that larvae collected in the offshore sites in the southern basin and those collected on the western side of Lake Michigan most likely hatched in the south eastern basin of Lake Michigan (Figure 10, 11). The exception to that pattern was at Manitowoc where larvae collected offshore most likely hatched on the eastern side of Lake Michigan north of Ludington (Figure 11). Larvae collected on the eastern side of Lake Michigan were modeled to hatch on the eastern side of Lake Michigan with predicted

trajectories both north and south of the collection location (Figure 12). No larval fish were predicted to hatch on the western side of Lake Michigan.

I found several environmental variables that were positively associated with increment width. As a fish ages, the increment width increases (Figure 13), indicating greater daily growth with increment age. Increasing zooplankton and detritus concentrations and warmer water temperatures were associated with larger increment widths (Figure 13). Based on the mixed model results, temperature, zooplankton concentration, detritus concentration, and age all had significant effects on otolith increment width (Table 1). There is a negative relationship between temperature and increment width when fish are age 3 (Table 1). The estimates from the mixed model show that when there is an interaction between age and detritus, zooplankton, and temperature, there is an increase in otolith increment width as the fish gets older. There is also an increase in growth rate when levels of zooplankton, detritus, temperatures increase (Figure 14).

Discussion

Favorable nursery habitat

The predicted hatch locations of larval alewife on the eastern side of Lake Michigan may indicate that the eastern side provided a more favorable nursery habitat than the western side for larval alewife in 2015. The dominant southwest wind across Lake Michigan causes persistent upwelling on the west and more frequent downwelling on the east. Upwelling is associated with colder water temperatures, which have a negative effect on alewife growth rate. Downwelling depresses the thermocline and is associated with warm surface temperatures. Metabolic rates of larval alewife increase with warming temperatures and larvae grow faster (Brown et al. 2004). Empirical studies of alewife in southwestern Lake Michigan indicated water temperatures were linked to hatch date and growth of alewife and warmer temperatures supported a favorable feeding environment with increased prey availability (Weber et al. 2015). Warmer spring-summer water temperatures also correspond to larger alewife year classes (O'Gorman et al. 2004; Madenjian et al. 2005), since larger fish have higher energy reserves and can survive the overwinter period (O'Gorman et al. 2004).

The sandy substrate on eastern side of Lake Michigan may promote primary and secondary production by limiting dreissenid mussel biomass, and better support prey for larval alewife. By 2000, dreissenid mussels invaded Lake Michigan and quickly became abundant in the nearshore area (Nalepa et al. 2009). Dreissenid mussels require a hard substrate for attachment in order to live in shallow, energetic locations. On the east side of Lake Michigan, the nearshore area is sandy, and does not support attachment of dreissenid mussels. In contrast, on the west side, the rocky nearshore area supports high biomass of attached dreissenid mussels (Karatayev et al. 2015). Dreissenid mussel filtration reduces phytoplankton biomass and primary production (Rowe et al., 2015; Kao et al., 2016).

Major tributary inputs on the eastern shore may support primary and secondary production and increase alewife growth rate. Several major tributaries including St. Joseph, Muskegon, Kalamazoo, and Grand Rivers flow to the eastern shore of Lake Michigan. Tributaries

carry nutrients, including phosphorous, and are influential in enrichment of the nearshore area (Bocaniov et al. 2013). Increased phosphorous loading increases phytoplankton biomass (Schelske et al. 2006). In 2015, the St. Joseph River had unusually high river discharge in July (USGS gauge data from https://waterdata.usgs.gov/usa/nwis/uv?site_no =04101500), increasing nutrient input into southeast Lake Michigan. The detritus variable in the biophysical model was produced by tributary inputs and zooplankton grazing, and was positively associated with larval growth rate. High detritus concentrations in the biophysical model may be indicative of more productive regions Lake Michigan, thus increasing prey availability for larval alewife.

It is unlikely that larval alewife only hatch on the eastern side of Lake Michigan. In the central western coast of Lake Michigan (Two Rivers, WI), Brandt et al. (1991) noted a large number of spawning alewife, and historically, alewife are known to spawn on both the eastern and western coasts of Lake Michigan (Goodyear et al. 1982). The samples of larvae I used for my analysis were surviving larvae at the time of collection, and it may be possible that larvae hatched on the western side may have experienced greater size-selective mortality; as previously noted, the eastern side may be more favorable for growth and survival. The predicted hatch locations also may be influenced by sampling bias in location or timing. Four of the six sampled transects were in the southern half of Lake Michigan and a large portion of the hatch regions are predicted to occur in the southern basin. Given that the southern basin exhibits its own gyre circulation, I expect dispersal of larvae to remain largely within the southern portion of the lake. This dispersal pattern has been shown in other studies. Beletsky et al. (2006) released drifters in the southern basin and the drifters remained mostly in the basin. There was one drifter that moved around the basin before moving north along the eastern shoreline, but the duration of the release was over 50 days long. Our oldest larva was 30 days and the majority were between 10 and 20 days old, so their horizontal movement is expected to be less. In another study, Beletsky et al. (2007) modeled yellow perch hatching in the southern basin and found that in June and July the particles remained in the basin and in August, they dispersed throughout the southern basin and into the eastern coastal region.

Study comparison

Results from this study both support and contrast results with previous work. Eppeheimer et al. (2019) performed an analysis to determine environmental influences on alewife growth rate using the same samples that were used in this study. Even though both studies explored the same question, my methods were largely different. Eppeheimer et al. (2019) collected temperature data at the sampling site and assumed that the surface temperature was representative of the temperatures experienced by larvae over their lifetime, but did not take into account transport history. Zooplankton data were collected at each sampling site during the tows and provided a limited view of the spatial variation inherent in zooplankton densities (Pothoven and Fahnenstiel 2015). My environmental data came from a biophysical model that produced hourly output, allowing us to track the environment over the course of the individual's life. Eppeheimer et al. (2019) also estimated average instantaneous larval growth rate (mm/day) by measuring the length of the fish (after correcting for shrinkage from preservation and subtracting the estimated hatch length) and dividing by the age. This

technique provided an average growth rate per day while our method measured the observed growth rate of larvae each day. Both studies found that age was a predictor of growth rate, but I found a monotonic increasing relationship, while Eppeheimer et al. (2019) found a non-linear relationship between age and growth rate. Other studies suggest a positive relationship between larval age and growth rate (Robert et al. 2007). I found a positive relationship between zooplankton concentration and alewife growth rate, a finding similar to Eppeheimer et al. (2019). Larval alewife consume zooplankton in Lake Michigan and higher densities of zooplankton were associated with increased growth rates. Höök et al. 2007 found alewife larvae had higher larval growth rates in drowned river mouth environments with small bodied zooplankton. The biophysical model does not represent zooplankton size, but can still be an indicator of potential prey density in an area. I found a significant positive effect of temperature on growth rate, but Eppeheimer et al. (2019) did not detect a temperature effect on larval growth rate. Insight into the transport of larval fish may have provided an improved indication of the role of temperature on growth rate over the life of a larval alewife.

Several studies have demonstrated a delay, or lag, in otolith response to environmental cues (Fey 2005; Pepin et al. 2001; Molony and Choat 1990). The delay in response time varies and may be species specific or related to other individual factors. Observed lag times between otolith growth and environmental cues include 6 days for the bridled monocle bream (Hall et al. 2019); 3 days in radiated shanny (Pepin et al. 2001), or even a range of 10-15 days for glass fish (Molony and Choat 1990), thus making the connection between otolith increments and environmental conditions somewhat ambiguous. Not all species exhibit such a lag and some species such as coregonids show an immediate otolith growth response to the environment (Eckmann and Ray 1986). I am not aware of any studies demonstrating the effect of the environment on alewife otolith increments, but if there is a lag, that would alter the results of the mixed model.

Model assessment with drifters

To use a single horizontal diffusion value for different spatial and temporal resolutions of Lake Michigan is to simplify the physical processes of the lake. I chose to use a value of 5.6 m^2 s^{-1} since this was realistic for southern Lake Michigan diffusivity (Thupaki et al. 2013). Yet, diffusion values have been shown to vary even when forcing and background conditions are similar (Choi et al. 2019). Lake circulation is driven by variable wind and as such, there is no set diffusion rate that can be applied to Lake Michigan. There are also differences in dispersal between dissolved substances such as alewife larvae and floating objects (drifters). Vertical shear affects dissolved substances but not floating objects (Choi et al. 2019), so I would expect the drifters to have lower dispersion compared with alewife larvae under observation. It may have improved accuracy to use a higher horizontal diffusivity value in the model to account for the differences in dispersal of surface drifters versus dissolved substances due to vertical shear. These results could indicate that the predicted hatch locations of larvae represent a low diffusivity scenario, representative of weaker wind forcing.

The currents between the points north and south of Ludington appear to be complex and challenging for the hydrodynamic model to simulate. The model predictions for drifters that

started slightly north of Ludington placed end locations of particles offshore (Figure 8) when the drifter trajectories exhibited alongshore coastal transport. Of the five scenarios modeled to track drifter movement between the two points north and south of Ludington, four inaccurately predicted the particles to move offshore instead of following the alongshore coastal transport exhibited by the drifters. The predictions of hatch location from alewife collected offshore of Ludington show higher dispersal and coastal transport compared with modeled drifter trajectories. The model trajectories were consistent with a northward coastal transport of larvae supported by previous studies (Carter and Haras 1985).

Conclusions

This study provides information on the physical transport of larval alewife and new insights on the influence of environmental conditions experienced in the early life stage of fish spawning in nearshore Lake Michigan. I was able to match daily larval growth with a date and predict the environmental exposure on that day, which supported my hypothesis that the daily growth rate of larval alewife can be predicted from their exposure to environmental conditions from hatch to capture. All of our sampled larvae were predicted to hatch along the eastern shore and may indicate that the eastern shore of Lake Michigan is a more favorable nursery habitat compared to the western shore. Environmental characteristics along the eastern shore include warmer water temperatures as a result of persistent southwest winds and downwelling, and increased nutrient input from high river discharge supporting primary and secondary production. Growth rate of fish during early life may contribute to year class success (Cowan and Shaw, 2002), and an early projection of alewife year class success could benefit management of salmonine species in Lake Michigan by informing salmonine stocking decisions. Future research that compared lake environments in weak and strong alewife recruitment years would be informative for understanding the contrasting environments that produce such year classes.

	Estimate	Std. Error	Pr(>|t|)
(Intercept)	1.365e+00	6.392e-02	<2e-16 ***
Age (days)	5.238e-02	7.054e-03	1.36e-12 ***
Temperature(°C)	-8.321e-02	2.035e-03	<2e-16 ***
Detritus (μg L^{-1})	-1.862e-04	3.307e-05	1.81e-08 ***
Zooplankton (μg L^{-1})	-1.504e-02	1.108e-03	<2e-16 ***
Age:Temperature	1.160e-02	1.645e-04	< 2e-16 ***
Age:Zooplankton	1.165e-03	7.594e-05	< 2e-16 ***
Age:Detritus	3.898e-05	3.399e-06	< 2e-16 ***

Table 1. Mixed effects model summary. One thousand particles were initiated for each of the 290 fish and subsamples of data were used from every 10th particle for each of the simulated fish. Hourly outputs for variables from the biophysical model were averaged over each day for each particle. Otolith increments were measured (μm). *** represents a level of significance with a p-value <0.001. An interaction of age with the environmental variables was included in the output. All variables were mean centered and estimate represents the slope of otolith increment width assuming all other variables are held at their mean value. Estimate represents change in otolith increment width (μm).
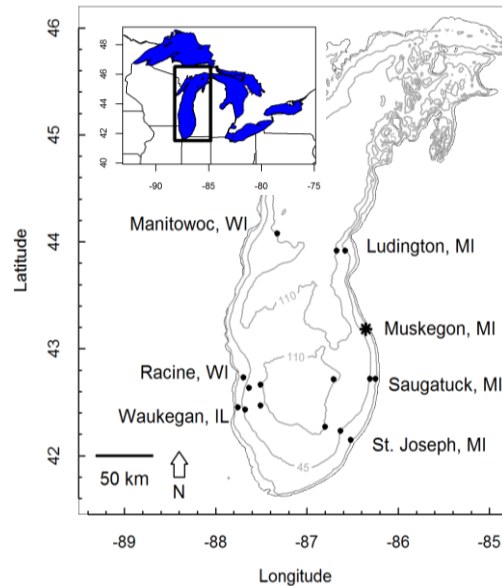
Fig. 1. Collection sites of larval alewife in Lake Michigan during the 2015 Cooperative Science and Monitoring Initiative (CSMI). Lake Michigan is located on the western side of Michigan and adjacent to Indiana, Illinois, and Wisconsin. It is one of the five Great Lakes. Black dots represent sampling sites along a transect and based off bathymetric contours (18-m, 46-m, and 91 or 110-m). Star is location of NOAA/National Data Buoy Center buoy 45161 off Muskegon, MI. Bathymetric contours depicted at 15-m, 45-m, and 110-m depicted.
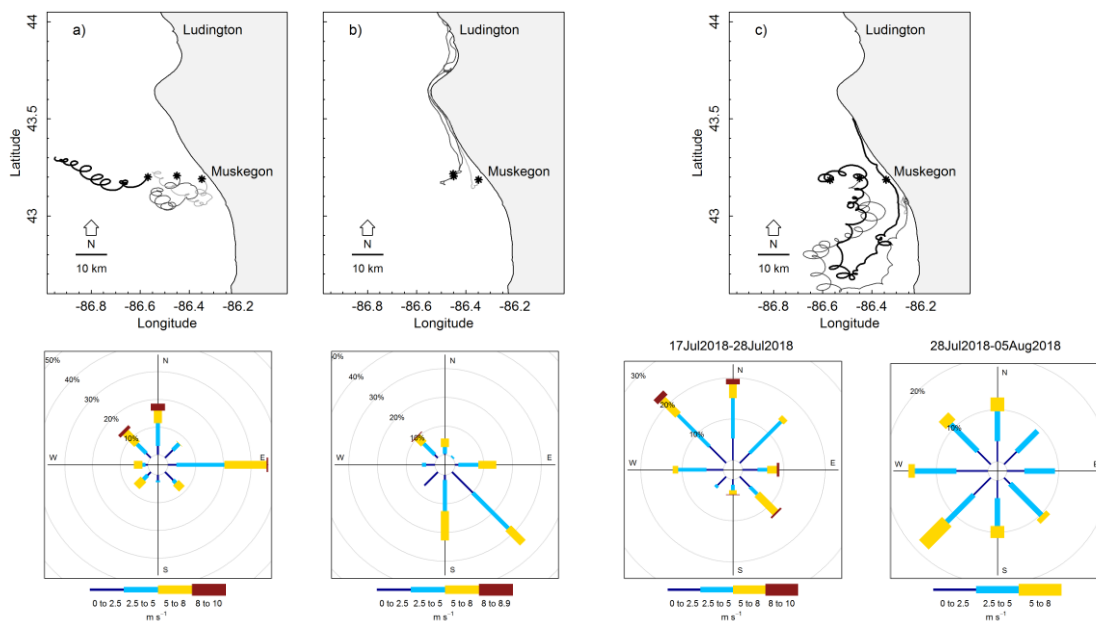
Fig. 2. Observed drifter tracks released on three separate occasions off the coast of Muskegon, MI. Stars represent the release site of drifters at M15, M45, and M110 (nearshore to offshore respectively).Site names represent bathymetric contours. a) First deployment drifters released June 5, 2018 and collected June 12, 2018. b) Second deployment drifters released June 27, 2018 at M15 and M45 with a third drifter released June 28, 2018 at M45 and all retrieved July 4, 2018 on shore c) Third deployment drifters released July 18, 2018 and collected August 5, 2018 on shore, drifters traveled south from July 18, 2018 to July 27, 2018, followed by a shift in direction July 27, 2018 to August 5, 2018. Wind rose plots depict wind speed and direction during the period of corresponding drifter deployments with wind data from NOAA/NDBC buoy 45161 located off Muskegon, MI. Wind rose plots for deployment 3 depict period July 17, 2018- July 26, 2018, when drifters traveled south and July 28, 2018-August 05, 2018, when drifters traveled north.
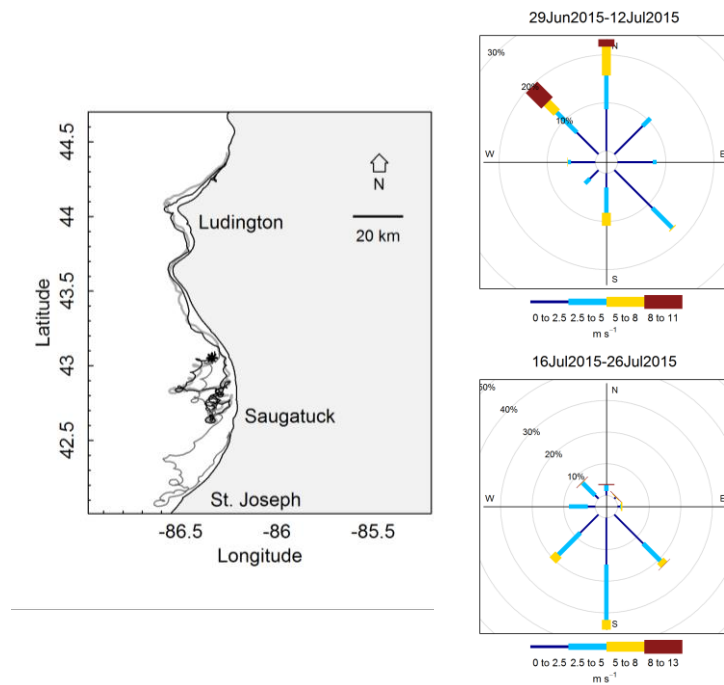
Fig. 3. Observed drifter tracks from three separate drifters deployed in Lake Michigan in 2015. The star symbol represents the release location. Drifters released simultaneously on June 30, 2015 and drifted for approximately one month with two traveling north and one moving south of the release location. Data source: Meng Xia, NOAA/University of Maryland. The wind rose plot depicts wind speed and direction during the period corresponding to longest deployed drifter with wind data from NOAA/NDBC buoy 45161 located off Muskegon, MI. Wind plots depict period of June 29, 2015 - July 12, 2015, when drifters traveled south and period of July 16, 2015 -July 26, 2015, when drifters traveled north.
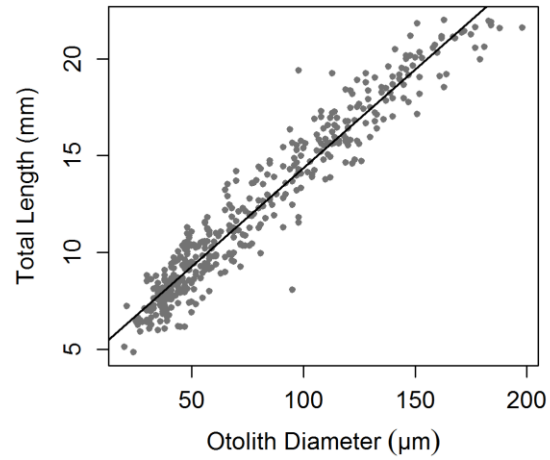
Fig. 4. Allometric relationship between otolith diameter (μm) and total length (mm) of larval alewife. R^2=0.9309; intercept=4.16; slope= 0.1017; n=290. Data source: Unpublished data from David Bunnell, USGS-GSLC.
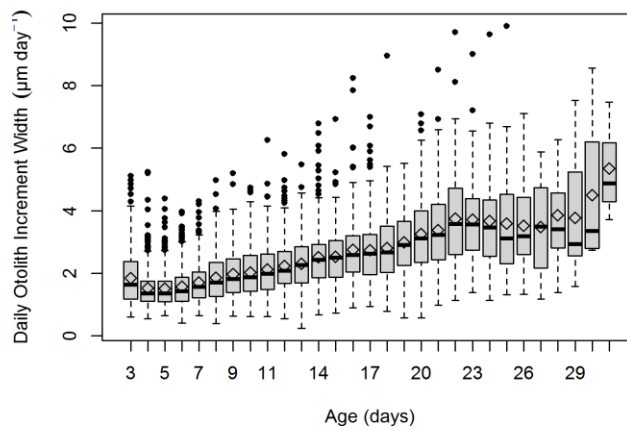

Fig. 5. Daily otolith increment width (μm/day) increases with the age of larvae (days). n=290. Diamonds are the mean daily increment width calculated for each age.
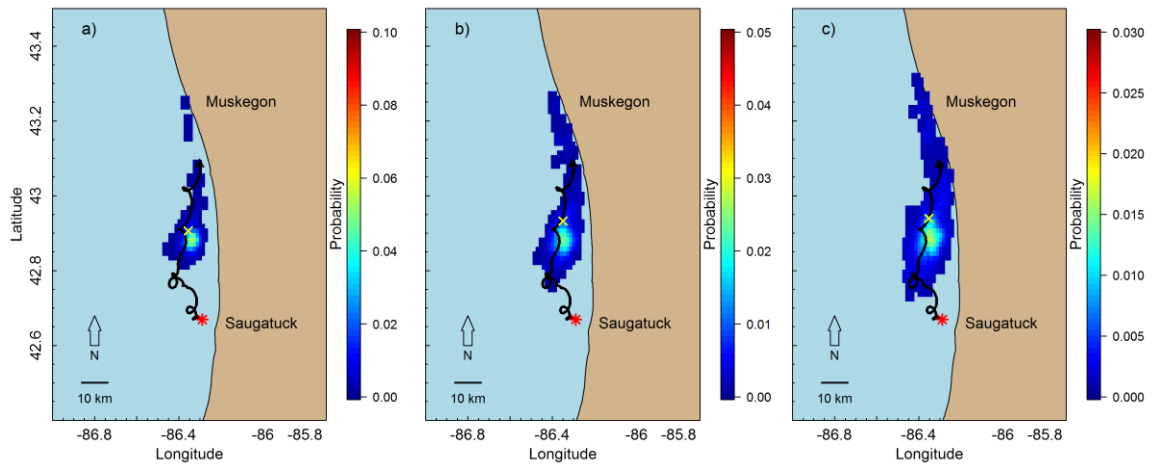
Fig. 6. Comparison of different horizontal diffusivity (K_H) (m^2 s^{-1}) values in model runs simulating a 2015 drifter release. Black triangle represents starting location of drifter and red star is ending location of drifter. The black line is the observed drifter trajectory. The yellow x represents the centroid of the predicted model results and measurements taken are distance (D) from centroid to drifter starting location. Probability represents the end location of 1000 simulated particles. a) K_H=1, D= 20.2 km; b) K_H=5, D=17.3 km; c) K_H=10, D=16.5 km. The upward velocity is 0.0003 m s^{-1} in all three comparisons. Simulations start July 7, 2015 and run backwards to June 30, 2015.
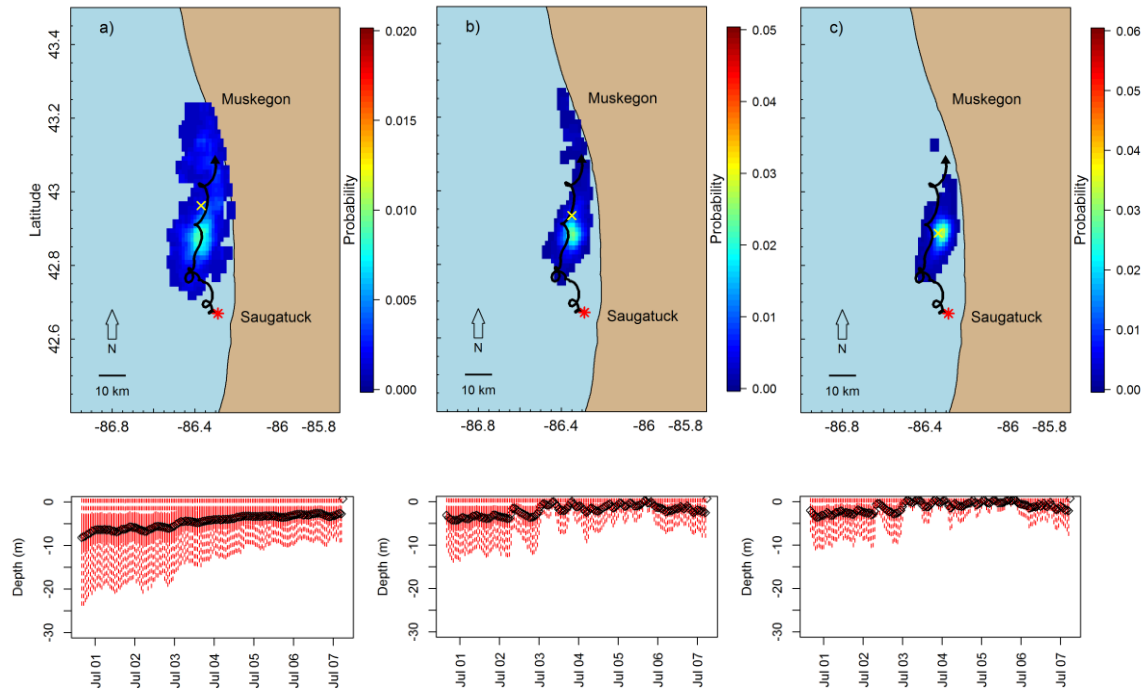
Fig. 7. Comparison of different vertical velocity values in model runs simulating 2015 drifter release. Black triangle represents starting location of drifter and red star is ending location of drifter. The black line is the observed drifter trajectory. The yellow x represents the centroid of the predicted model results and measurements taken are distance (D) from centroid to drifter starting location. Probability represents the end location of 1000 simulated particles. Boxplots represent depth (m) of 1000 particles from the surface over the duration of the simulation period; the black diamond represents the mean depth each hour. Model simulations start on July 7 and run backwards to June 30. The horizontal diffusivity is set to 5 m^2 s^{-1} in scenarios. a) Vertical velocity=0 m s^{-1}, D=13.6 km; b) vertical velocity =0.0003 m s^{-1}, D=17.3 km; c) vertical velocity= 0.001 m s^{-1}, D=22.0 km.
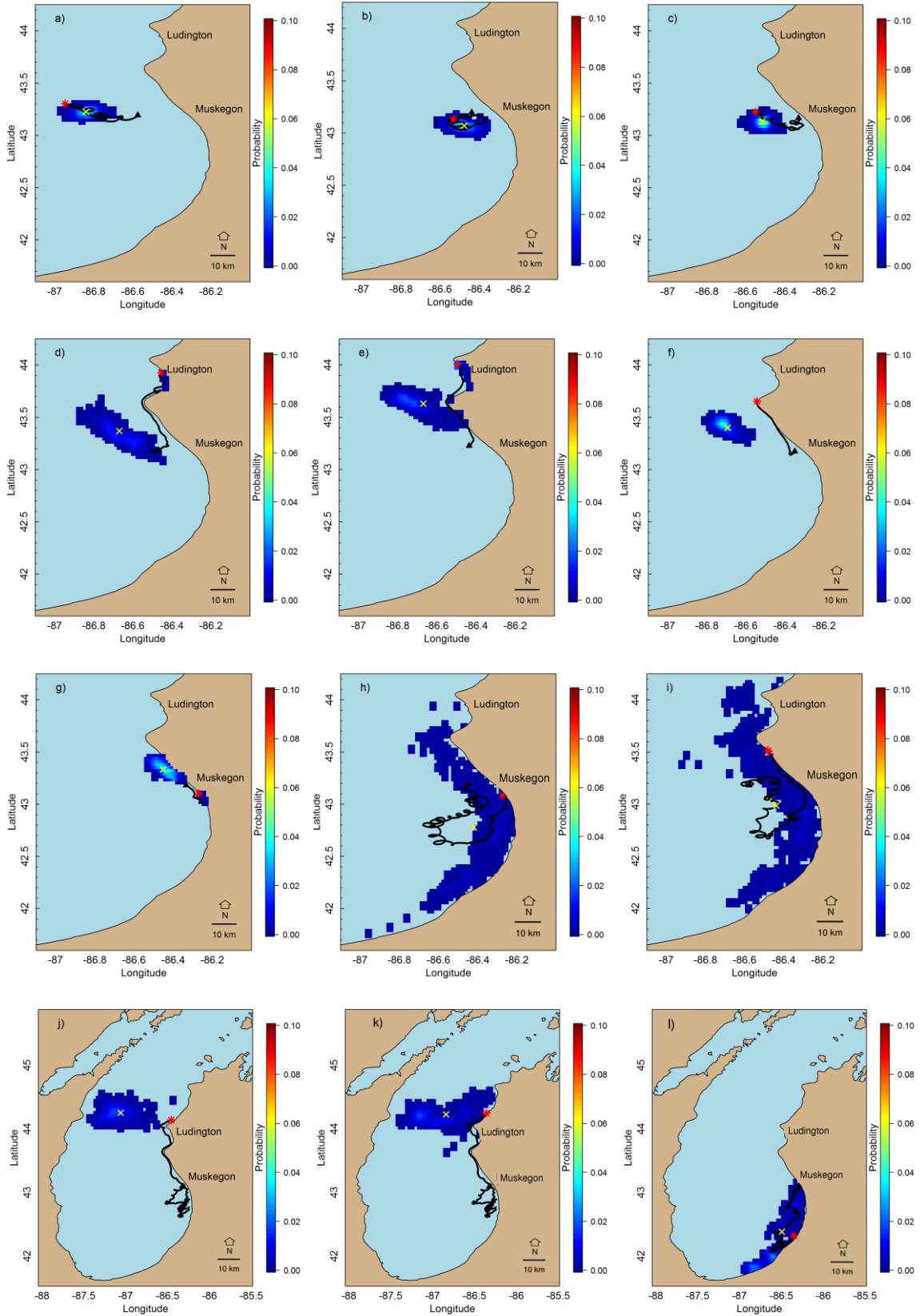
Fig. 8. Model estimates from 2018 and 2015 drifter observations. Simulations were run with an upwards velocity of 0.0003 m s^{-1} and K_H of 5.6 m^2 s^{-1}. The black triangle represents the starting location of drifter and the red star is the end location of the drifter. The black line is the observed drifter trajectory. One thousand particles were initiated at the end location of the drifter observations and a backwards-trajectory was applied. The yellow x represents the centroid of the predicted model results and measurements taken are distance (D) from centroid to drifter starting location. a-c) Deployment 1 in 2018 at M110 D= 21.5 km, M45 D= 14.1 km, and M15 D= 15.7 km respectively; d-f) Deployment 2 in 2018 at M45 D= 26.0 km, M45 D= 48.9 km and M15 D= 37.6 km respectively; g-i) Deployment 3 in 2018 at M15 D= 19.5 km, M45 D= 45.9 km, and M110 D= 25.4 km respectively; j-l) Deployment in 2015 with 3 separate drifters released off Muskegon, MI on June 30, 2015 D=138.4 km, D=127.4 km, and D= 79.3 km respectively.
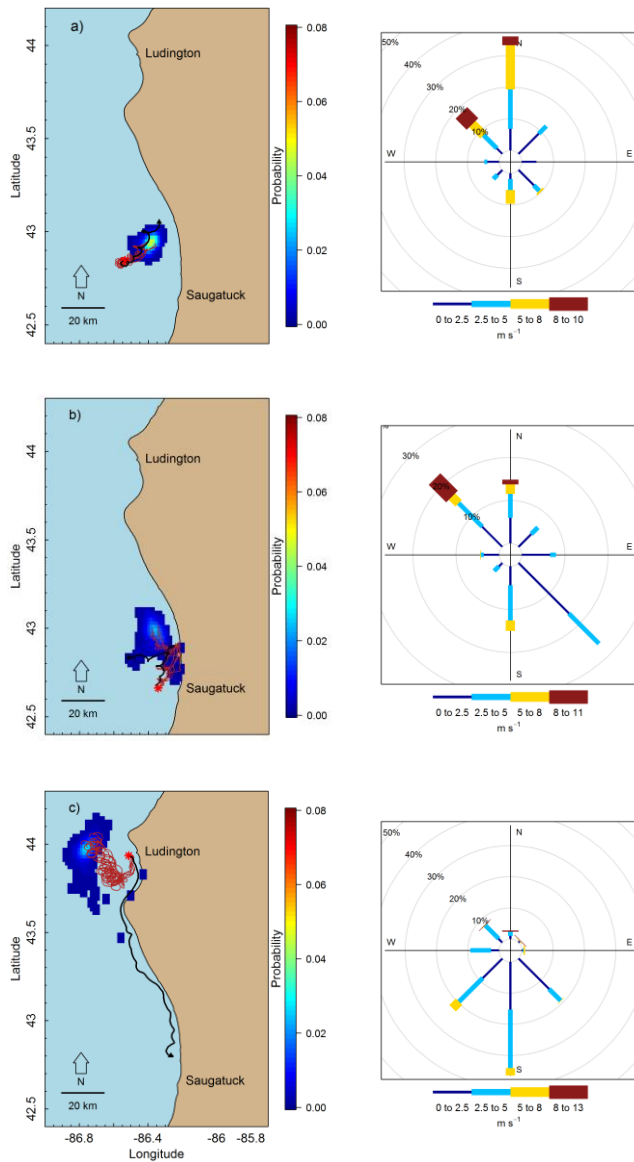
Fig. 9. Observed vs. model predictions for various transport scenarios in 2015. Drift patterns were characterized by a) near inertial oscillations; b) large directional change in current with near inertial oscillations; c) alongshore current. Red lines represent a randomly selected subset of the 1000 particles simulated in the model. The yellow star is the starting location for modeled backwards trajectory run and end location of observed drifter tracks. Probability represents the end location of 1000 simulated particles. The black dot is the starting location of the drifter. Horizontal diffusivity is 5.6 $m^2 s^{-1}$ and upwards velocity is 0.0003 $m s^{-1}$. Dates of drifter release were a) June 30, 2015 -July 04, 2015; b) July 04, 2015 - July 09, 2015; c) July 17, 2015 - July 26, 2015. Corresponding wind rose plots include 24 hours prior to the period of drifter release with data derived from daily buoy observations (NDBC 45161) off Muskegon, MI.
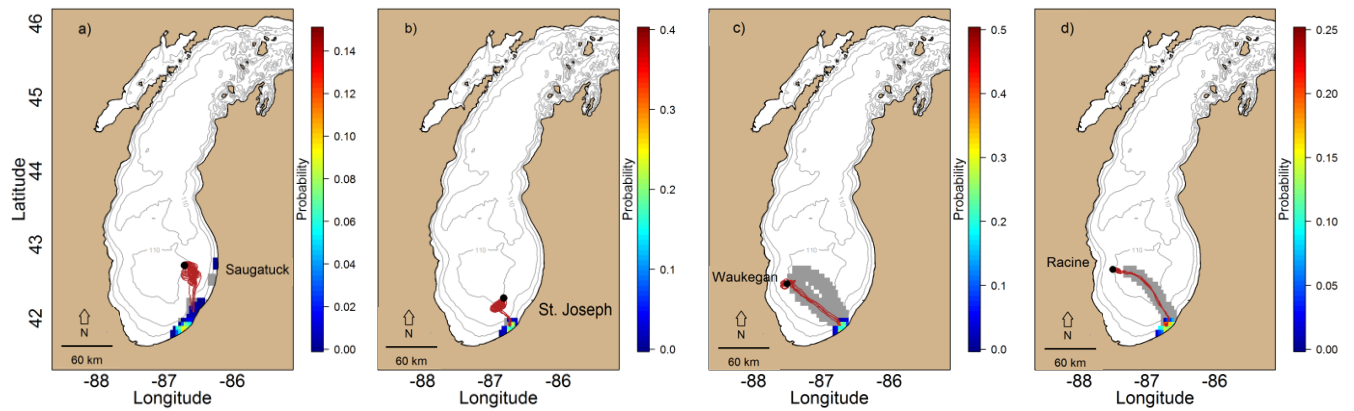
 Fig. 10. Estimated probability of hatch locations at offshore collection sites in the southern half of Lake Michigan. The grey area represents predicted hatch location in bathymetric depths >20-m. Probability represents predicted hatch location in bathymetric depths < 20-m of all samples collected at a) Saugatuck 110-m on July 16, 2015; b) St. Joseph 110-m on July 19, 2015; c) Waukegan 91-m on July 21, 2015; d) Racine 91-m on July 23. 2015. Red lines represent the trajectories of five particles from the model simulations.
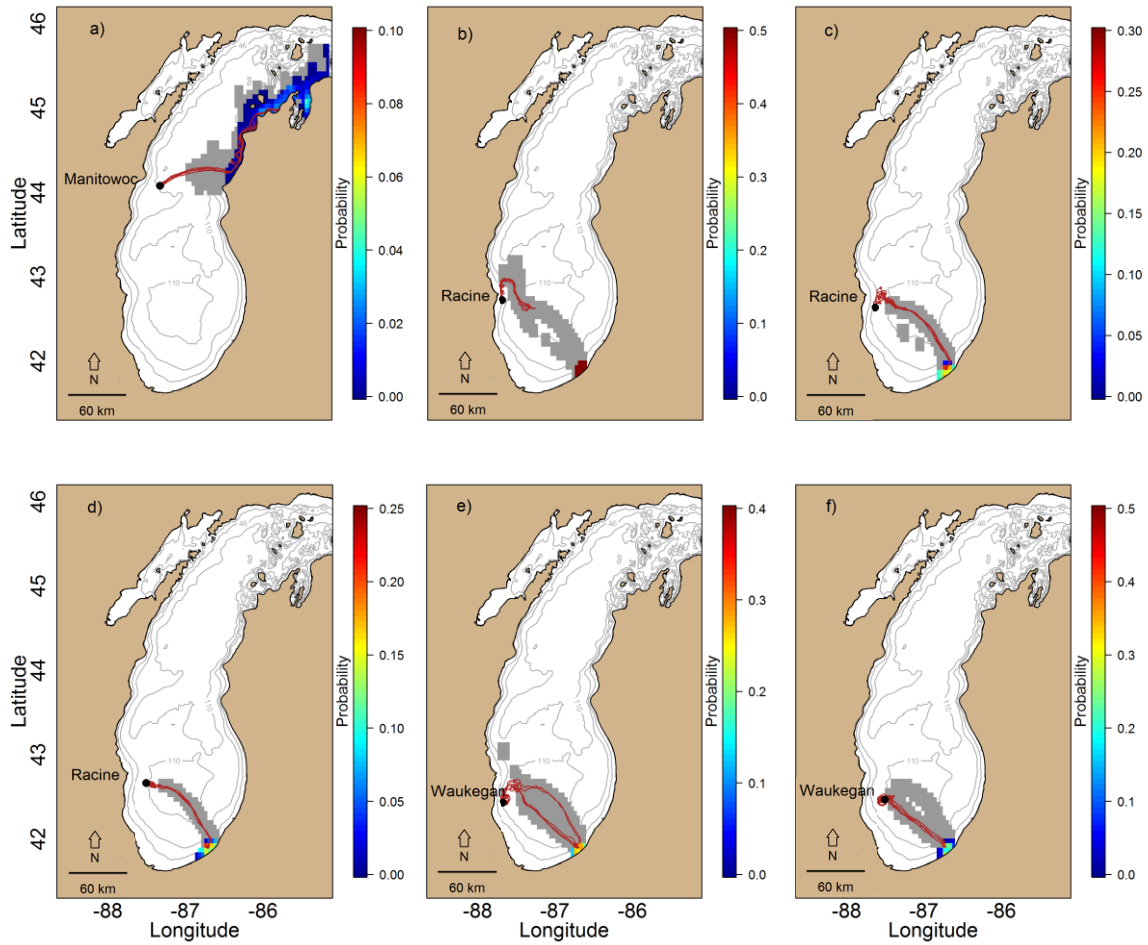
Fig. 11. Comparison of hatch locations for western Lake Michigan larval collection sites. The grey area represents predicted hatch locations in bathymetric depth >20-m. Probability represents predicted hatch locations in bathymetric depths < 20-m of all samples collected at a) Manitowoc 110-m on July 24, 2015; b) Racine 18-m on July 22, 2015; c) Racine 46-m on July 22, 2015; d) Racine 91-m on July 23, 2015; e) Waukegan 46-m on July 20, 2015; f) Waukegan 91-m on July 21, 2015. Red lines represent the trajectory of five randomly selected particles from the model simulations.
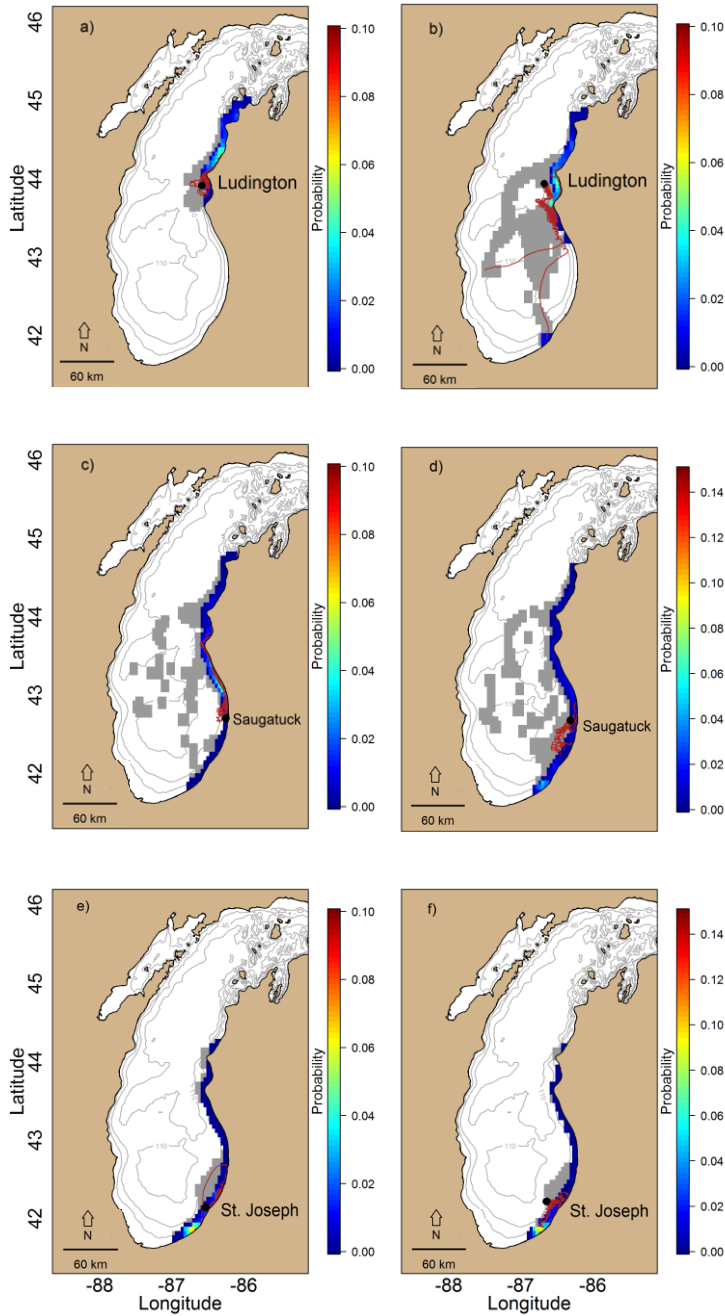
Fig. 12. Comparison of estimated hatch locations at eastern Lake Michigan collection sites. The grey area represents predicted hatch locations in bathymetric depths >20-m. Probability represents predicted hatch locations in bathymetric depths < 20-m of all samples collected at a) Ludington 46-m on July 11, 2015; b) Ludington 110-m on July 12, 2015; c) Saugatuck 18-m on July 12, 2015; d) Saugatuck 46-m on July 13, 2015; e) St. Joseph 18-m on July 18, 2015; f) St. Joseph 46-m on July 16, 2015. Red lines represent the trajectory of five randomly selected particles from the model simulations.
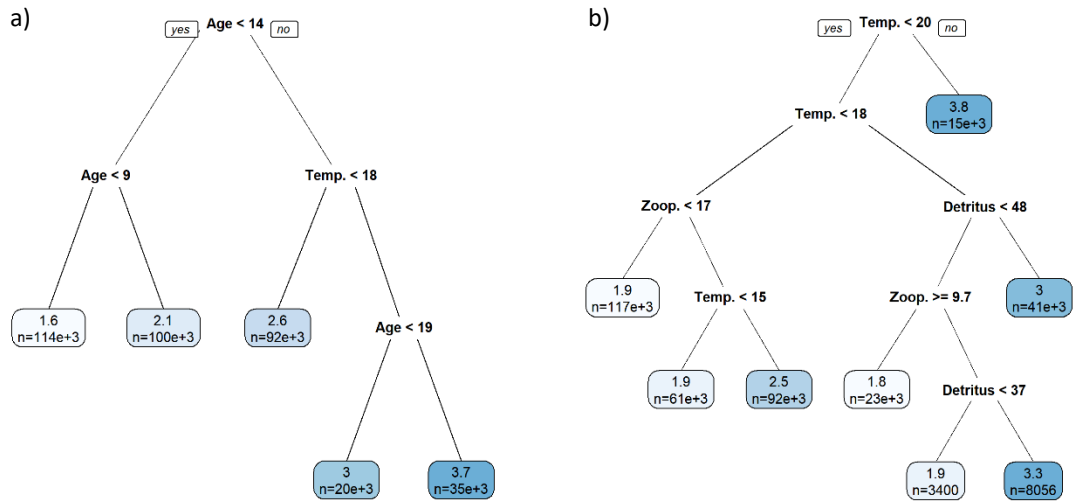
Fig. 13. Regression trees of environmental predictors and their influence on otolith increment width. Intensity of node color is proportional to the otolith increment width value predicted at the node based upon environmental variables. Sample size for each argument = *n*. a) regression tree using age, zooplankton, phytoplankton, temperature, and detritus as predictor variables; b) regression tree using zooplankton, phytoplankon, temperature, and detritus as predictor variables.
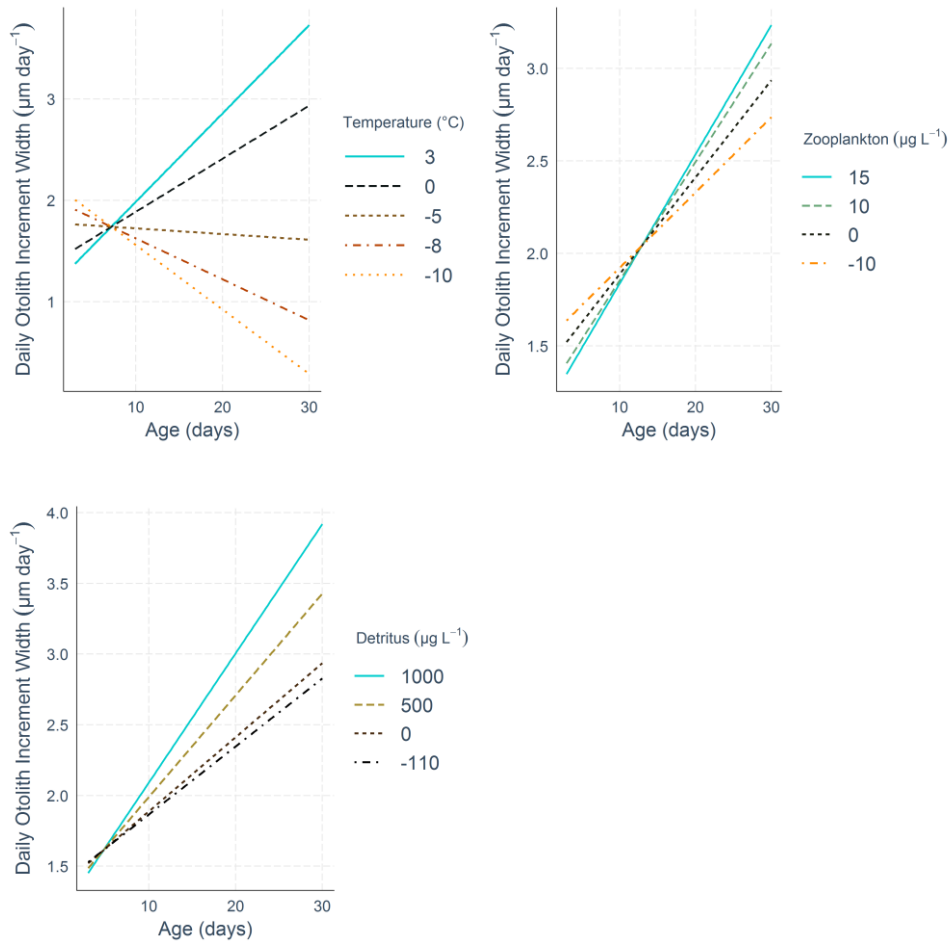
Fig. 14. Linear mixed effects model results from biophysical model data. One thousand particles were initiated for each of the 290 larvae and subsamples of data were taken at every 10th particle for each larvae. Hourly output of variables were averaged over each day for each particle. An interaction of age was included with each variable. All variables are mean centered with zero representing the mean value of each variable. Mean temperature=16.864 °C, mean detritus=147.645 µg L^{-1}, mean zooplankton=17.309 µg L^{-1}.
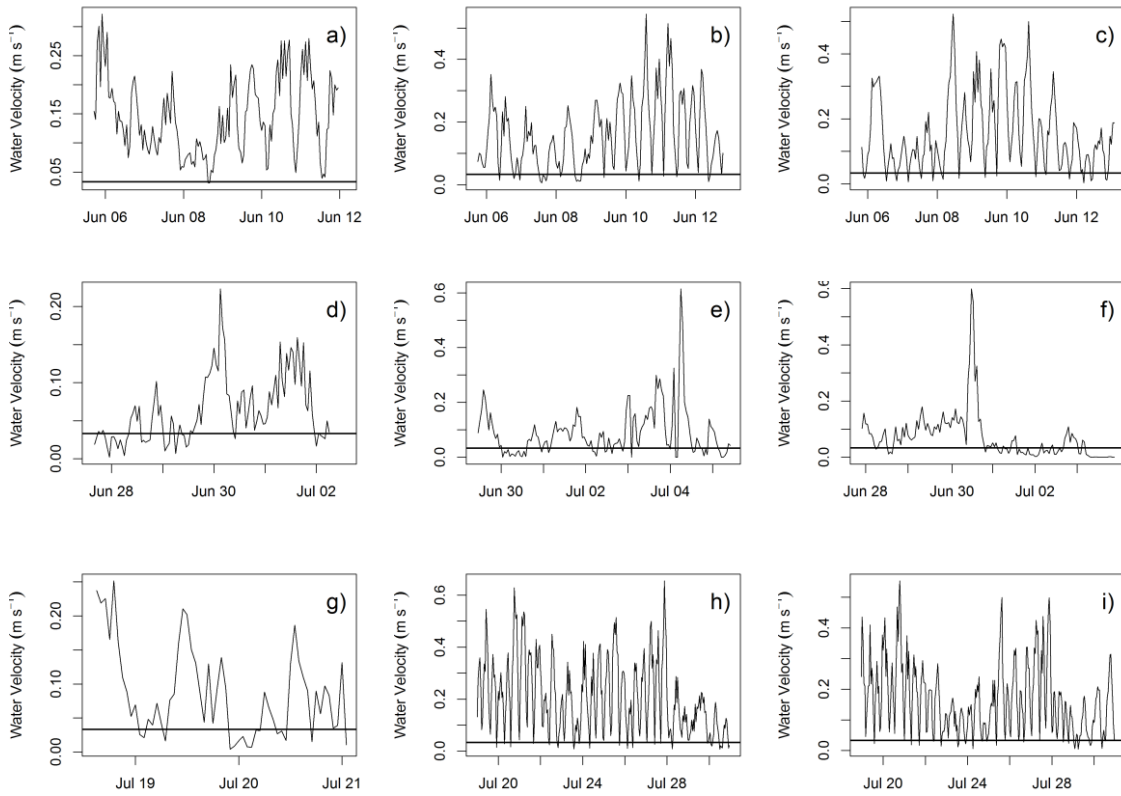
Supplemental Figures

Fig. S1. Calculated water velocity for the 2018 drifter deployments. a-c) deployment 1 at M15, M45, M110 respectively; d-f) deployment 2 M15, M45, M45 respectively. g-i) deployment 3 at M15, M45, M110 respectively. Site names represent bathymetric controus at 15-m, 45-m, and 110-m. Horizontal line at 0.033 m s^{-1} represents estimated larval alewife (22 mm TL) swim

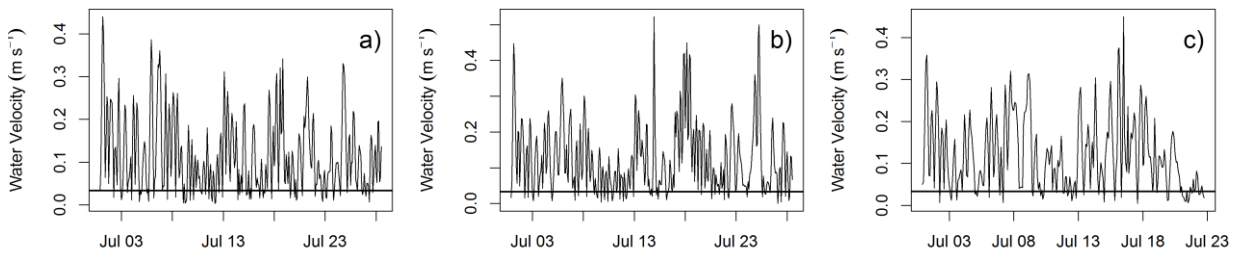

Fig. S2. Calculated water velocity for the 2015 drifter deployments. Horizontal line at 0.033 m s^{-1} represents estimated larval alewife (22 mm TL) swim speed. a,c) drifters traveled north; b) drifter traveled south of starting location.

References

Anderson, E.J., and Schwab, D.J. 2013. Predicting the oscillating bi-directional exchange flow in the Straits of Mackinac. J. Great Lakes Res. **39**(4): 663–671. doi:10.1016/j.jglr.2013.09.001.

Anderson, E.J., and Schwab, D.J. 2017. Meteorological influence on summertime baroclinic exchange in the Straits of Mackinac. J. Geophys. Res. **122**(3): 2171-2182. doi:10.1002/2016JC012255.

Ashworth, E.C., Hall, N.G., Hesp, S.A., Coulson, P.G., and Potter, I.C. 2017. Age and growth rate variation influence the functional relationship between somatic and otolith size. Can. J. Fish. Aquat. 74(5): 680. doi:10.1139/cjfas-2015-0471.

Bai, X., Wang, J., Schwab, D.J., Yang, Y., Luo, L., Leshkevich, G.A., and Liu, S. 2013. Modeling 1993-2008 climatology of seasonal general circulation and thermal structure in the Great Lakes using FVCOM. Ocean Model. **65**: 40-63. doi:10.1016/j.ocemod.2013.02.003.

Beletsky, D., Saylor, J.H., and Schwab, D.J. 1999. Mean circulation in the Great Lakes. J. Gt. Lakes Res. **25**: 78-93.

Beletsky, D., and Schwab, D.J. 2001. Modeling circulation and thermal structure in Lake Michigan: Annual cycle and interannual variability. J. Geophys. Res. 106(C9): 19745-19771. doi: 10.1029/2000JC000691.

Beletsky, D., Schwab, D.J., Mason, D.M., Rutherford, E., McCormick, M.J., Vanderploeg, H.A., and Janssen, J. 2004. Modeling the transport of larval yellow perch in Lake Michigan. *In* Estuarine and Coastal Modeling, the 8th International Conference, November 3–5, 2003, Monterey, CA. *Edited* by M.L. Spaulding. American Society of Civil Engineers, Reston, VA. pp. 439–454.

Beletsky, D., Schwab, D., and McCormick, M. 2006. Modeling the 1998-2003 summer circulation and thermal structure in Lake Michigan. J. Geophys. Res. **3**(C10): C10010. doi:10.1029/2005JC003222.

Beletsky, D., Mason, D.M., Schwab, D.J., Rutherford, E.S., Janssen, J., Clapp, D.F., and Dettmers, J.M. 2007. Biophysical model of larval yellow perch advection and settlement in Lake Michigan. J. Gt. Lakes Res. **33**: 842-866. doi:10.3394/0380-1330(2007)33[842:BMOLYP]2.0.CO;2.

Beletsky, D., Beletsky, R., Rutherford, E.S., Sieracki, J.L., Bossenbroek, J.M., Chadderton, W.L., Wittmann, M.E., Annis, G.M., and Lodge, D.M. 2017. Predicting spread of aquatic invasive species by lake currents. J. Gt. Lakes Res. **43**: 14-32. doi:10.1016/j.jglr.2017.02.001.

Benjamin, S.G., Weygandt, S.S., Brown, J.M., Hu, M., Alexander, C.R., Smirnova, T.G., Olson, J.B., James, E.P., Dowell, D.G., Grell, G.A., Lin H., Peckham, S.E., Smith, T.L., Moninger, W.R., Kenyon, J.S., and Manikin, G.S. 2016. A North American hourly assimilation and model

forecast cycle: The Rapid Refresh. Mon. Weather Rev. **144**(4): 1669-1694. doi:10.1175/MWR-D-15-0242.1.

Brandt, S.B., Mason, D.M., Patrick, E.V., Argyle, R.L., Wells, L., Unger, P.A., and Stewart, D.J. 1991. Acoustic measures of the abundance and size of pelagic planktivores in Lake Michigan. Can. J. Fish. Aquat. **48**: 894-908. doi:10.1139/f91-106.

Brodnik, R.M., Fraker, M.E., Anderson, E.J., Carreon-Martinez, L., DeVanna, K.M., Heath, D.D., Reichert, J.M., Roseman, E.F., and Ludsin, S.A. 2015. Larval dispersal underlies demographically important intersystem connectivity in a Great Lakes yellow perch (*Perca flavescens*) population. Can. J. Fish. Aquat. Sci. **73**: 416-426. doi:10.1139/cjfas-2015-0161.

Brown, J.H., Gillooly, J.F., Allen, A.P., Savage, V.M., and West, G.B. 2004. Toward a metabolic theory of ecology. Ecology. **85**: 1771–1789. doi:10.1890/03-9000.

Bunnell, D.B., Barbierdo, R.P., Ludsin, S.A., Madenjian, C.P., Warren, G.J., Dolan, D.M., Brenden, T.O., Briland, R., Gorman, O.T., He, J.X., Johengen, T.H., Lantry, B.F., Lesht, B.M., Nalepa, T.F., Riley, S.C., Riseng, C.M., Tresja, T.J., Tsehaye, I., Walsh, M.G., Warner, D.M., and Weidel, B.C. 2014. Changing ecosystem dynamics in the Laurentian Great Lakes: Bottom-up and top-down regulation. BioScience **64**: 26-39. doi:10.1093/ biosci/bit001.

Caló, A., Lett, C., Mourre, B., Pérez-Ruzafa, A., and García-Charton, J.A. 2018. Use of Lagrangian simulations to hindcast the geographical position of propagule release zones in a Mediterranean coastal fish. Mar. Environ. Res. **134**: 16-27. doi:10.1016/j.marenvres.2017.12.011.

Carrick, H.J., Barbiero, R.P., Tuchman, M. 2019. Variations in Lake Michigan phytoplankton: Temporal, spatial, and historical trends. J. Gt. Lakes Res. **27**(4): 467-485. doi:10.1016/S0380-1330(01)70661-2.

Carter, C.H., and Haras, W.S. 1985. Great Lakes. *In* The World's Coastline. *Edited by* E.C.F. Bird and M.C. Schwartz. VanNostrand Reinhold, New York. pp. 253-260.

Chen, C., Beardsley, R.C., and Cowles, G. 2006. An unstructured grid, finite-volume coastal ocean model (FVCOM) system. Oceanogra. **19**(1): 78–89. doi:10.5670/oceanog.2006.92.

Choi, J.M., Troy, C., Hawley, N., McCormick, M., and Wells, M. 2019. Lateral dispersion of dye and drifters in the center of a very large lake. Limnology and Oceanography (In Press)

Churchill, J.H., Runge, J. and Chen, C. 2011. Processes controlling retention of spring-spawned Atlantic cod (*Gadus morhua*) in the western Gulf of Maine and their relationship to an index of recruitment success Fish. Oceanogr. 20(1): 32–46. doi:10.1111/j.1365-2419.2010.00563.x.

Clark, R.D., Bence, J.R., Claramunt, R.M., Clevenger, J.A., Kornis, M.S., Bronte, C.R., Madenjian, C.P., and Roseman, E.F. 2017. Changes in movements of chinook salmon between lakes

Huron and Michigan after alewife population collapse. North Am. J. Fish. Manage. **37**(6): 1311-1331. doi:10.1080/02755947.2017.1378778.

Collingsworth, P.D., Bunnell, D.B., Madenjian, C.P., and Riley, S.C. 2014. Comparative recruitment dynamics of alewife and bloater in lakes Michigan and Huron. Trans. Am. Fish. So. **143**: 294-309. doi:10.1080/00028487.2013.833986.

Cowan, J.H., and Shaw, R.F. 2002. Recruitment. *In* Fishery science: the unique contributions of early life stages. *Edited by* L.A. Fuiman and R.G. Werner. Blackwell Science, Oxford, UK. pp. 88-111.

Cury, P. and Roy, C. 1989. Optimal environmental window and pelagic fish recruitment success in upwelling areas. Can. J. Fish. Aquat. Sci. **46**(4): 670-680. doi:10.1139/f89-086.

Cushing, D.H. 1990. Plankton production and year-class strength in fish populations–an update of the match mismatch hypothesis. Adv. Mar. Biol. **26**:249–293. doi:10.1016/S0065-2881(08)60202-3.

Dettmers, J.M., Janssen, J., Pientka, B., Fulford, R.S., and Jude, D.J. 2005. Evidence across multiple scales for offshore transport of yellow perch *(Perca flavescens)* larvae in Lake Michigan. Can. J. Fish. Aquat. Sci. **62**: 2683–2693. doi:10.1139/f05-173.

Dunlop, E.S., and Riley, S.C. 2013. The contribution of cold winter temperatures to the 2003 alewife population collapse in Lake Huron. J. Gt. Lakes Res. **39**(4): 682-689. doi:10.1016/j.jglr.2013.08.001.

Dolan, D.M., and Chapra, S.C. 2012. Great Lakes total phosphorus revisited: 1. Loading analysis and update (1994–2008). J. Great Lakes Res. **38**: 730–740. doi:10.1016/j.jglr.2012.10.001.

Edsall, T.A. 1970. The effect of temperature on the rate of development and survival of alewife eggs and larvae. Trans. Am. Fish. So. **99**(2): 376-380. doi:10.1577/1548-8659(1970)99<376:TEOTOT>2.0.CO;2.

Eggold, B., Gorenflo, T., Price, J., Santucci, V., and Wesley, J. 2018. Lake Michigan salmonine stocking strategy, November 2018. Lake Michigan Committee, Great Lakes Fishery Commission, Ann Arbor, Mich. pp. 1-11.

Eckmann, R. and Ray, P. 1987. Daily increments on the otoliths of larval and juvenile *Coregonus* spp., and their modification by environmental factors. Hydrobiologia. 148(2): 137-143. doi:10.1007/BF00008399.

Eppehimer, D.E., Bunnell, D.B., Armenio, P.M., Warner, D.M., Eaton, L.A., Wells, D.J., Rutherford, E.S. 2019. Densities, diets, and growth rates of larval alewife and bloater in a changing Lake Michigan ecosystem. Trans. Am. Fish. So. **148**(4): 755-770. doi:10.1002/tafs.10171.

Essig, R.J., and Cole, C.F. 1986. Methods of estimating larval fish mortality from daily increments in otoliths. Trans. Am. Fish. So. **115**(1): 34-40. doi:10.1577/1548-8659(1986)115<34:MOELFM>2.0.CO;2.

Fahnenstiel, G.L., Chandler, J.F., Carrick, H.J., and Scavia, D. 1989. Photosynthetic characteristics of phytoplankton communities in Lakes Huron and Michigan: P-I parameters and end-products. J. Great Lakes Res. **15**: 394–407. doi:10.1016/S0380-1330(89)71495-7.

Fey, D.P. 2005. Is the marginal otolith increment width a reliable recent growth index for larval and juvenile herring? J. Fish Biol. **66** 1692-1703. doi:10.1111/j.1095-8649.2005.00716.x.

Goodyear, C.D., Edsall, T.A., Ormsby Dempsey, D.M., Moss, G.D., and Polanski, P.E. 1982. Atlas of the spawning and nursery areas of Great Lakes fishes. US Fish and Wildlife Service, Washington, D.C. FWS/OBS-82/52.

Hall, A.E., Vitale, L., and Kingsford, M.J. 2019. Planktonic larval duration, early growth, and the influences of dietary input on the otolith microstructure of *Scolopsis bilineatus* (Nemipteridae). Environ. Biol. Fish. **102**: 541-522. doi:10.1007/s10641-019-00852-z.

Heufelder, G.R., Jude, D., and Tesar, F.J. 1982. Effects of upwelling on local abundance and sistribution of larval alewife (*Alosa pseudoharengus*) in eastern Lake Michigan. Can. J. Fish. Aquat. Sci. **39**(11): 1531-1537. doi:10.1139/f82-205.

Hjort, J. 1914. Fluctuations in the great fisheries of northern Europe: viewed in the light of biological research. In Rapports Et Procés-verbaux Des Réunions. **20**: 1–228.

Höök, T.O., McCormick, M.J., Rutherford, E.S., II, Mason, D.M., and Carter, G.S. 2006. Short term water mass movement in Lake Michigan: Implications for larval fish transport. J. Gt. Lakes Res. **32**(4): 728-737. doi:10.3394/0380-1330(2006)32[728:SWMMIL]2.0.CO;2.

Höök, T.O., Rutherford, E.S., II, Mason, D.M., and Carter, G.S. 2007. Hatch Dates, growth, survival, and overwinter mortality of age-0 alewives in Lake Michigan: Implications for habitat-specific recruitment success. Trans. Am. Fish. So. **136**: 1298-1312. doi:10.1577/T06-194.1.

Houde, E.D. 2002. Mortality. *In* Fishery science: the unique contributions of early life stages. *Edited by* L.A. Fuiman and R.G. Werner. Blackwell Science, Oxford, UK. pp. 64–87.

Huret, M., Runge, J.A., Chen, C., Cowles, G., Xu, Q., and Pringle, J.M. 2007. Dispersal modeling the fish early life stages: Sensitivity with application to Atlantic cod in the western Gulf of Maine. Mar. Ecol. Prog. Ser. **347**: 261-274. doi:10.3354/meps06983.

Johnson, J.E., DeWitt, S.P., and Gonder, D.J.A. 2010. Mass marking reveals emerging self-regulation of the Chinook Salmon population in Lake Huron. North Am. J. Fish. Manage. **30**: 518–529. doi:10.1577/M09-094.1.

Kao, Y., Adlerstein, S.A., and Rutherford, E.S. 2016. Assessment of top-down and bottom-up controls on the collapse of alewives *(Alosa pseudoharengus)* in Lake Huron. Ecosystems. **19**(5): 803-831. doi:10.1007/s10021-016-9969-y.

Karatayev, A.Y., Burlakova, L.E., and Padilla, D.K. 2015. Zebra versus quagga mussels: a review of their spread, population dynamics, and ecosystem impact. Hydrobiologia. **746**: 97-112. doi:10.1007/s10750-014-1901-x.

Klumb, R.A., Rudstam, L.G., and Mills, R.L. 2003. Comparison of alewife young of the year and adult respiration and swimming speed bioenergetics model parameters: Implications of extrapolation. Trans. Am. Fish. So. **132**(6): 1089-1103. doi:10.1577/T03-038.

Kuznetsova, A., Brockhoff, P.B., Christensen, R.H.B. 2017. lmerTest Package: Tests in Linear Mixed Effects Models. J. Stat. Softw. **82**(13): 1-26. doi:10.18637/jss.v082.i13.

LaBay, S.R., and Lauer, T.E. 2006. An evaluation of the accuracy of age estimation methods for southern Lake Michigan Alewives. North Am. J. Fish. Manage. **26**: 571-579. doi:10.1577/M05-098.1.

Lasker, R. 1978. The relation between oceanographic conditions, and larval anchovy food in the California Current: identification of factors contributing to recruitment failure. Rapp. P.-V. Reun. Cons. Int. Explo. Mer. **173**: 212–230.

Long, J.A. 2019. *interactions: Comprehensive, User-Friendly Toolkit for Probing Interactions.* R package version 1.1.0. https://cran.r-project.org/package=interactions.

Lohrenz, S.E., Fahnenstiel, G.L., Millie, D.F., Schofield, O.M., Johengen, T., and Bergmann, T. 2004. Spring phytoplankton photosynthesis, growth, and primary production and relationships to a recurrent coastal sediment plume and river inputs in southeastern Lake Michigan. J. Geophys. Res. **109**: C10S14. doi:10.1029/2004JC002383.

Ludsin, S.A., DeVanna, K.M., and Smith, R.E.H. 2014. Physical-biological coupling and the challenge of understanding fish recruitment in freshwater lakes. Can. J. Fish. Aquat. Sci. **71**: 775-794. doi:10.1139/cjfas-2013-0512.

Madenjian, C.P., and Jude, D.J. 1985. Comparison of sleds versus plankton nets for sampling fish larvae and eggs. Hydrobiologia. **124**(3): 275-281. doi:10.1007/BF00015245.

Madenjian, C.P., Höök, T.O., Rutherford, E.S., Mason, D.M., Croley, T.E., II, Szalai, E.B., and Bence, J.R. 2005. Recruitment variability of alewives in Lake Michigan. Trans. Am. Fish. Soc. **134**: 218–230. doi:10.1577/FT03-222.1.

Madenjian, C.P. Bunnell, D.B., Warner, D.M., Pothoven, S.M., Fahnenstiel, G.L., Nalepa, T.F., Vanderploeg, H.A., Tsehaye, I., Claramunt, R.M., and Clark, R.D. 2015. Changes in the Lake Michigan food web following dreissenid mussel invasions: A synthesis. J. Gt. Lakes Res. **41**(3): 217-231. doi:10.1016/j.jglr.2015.08.009.

Madenjian, C.P., Bunnell, D.B., Desorcie, T.J., Armenio, P., and Adams, J.V. 2017. Status and trends of prey fish populations in Lake Michigan, 2017. Compiled Reports to the Great Lakes Fishery Commission of the Annual Bottom Trawl and Acoustics Survey, 2017. Great Lakes Fishery Commission, Ann Arbor, Mich. pp. 12-28.

Martin, B.T., Czesny, S.J., and Wahl, D.H. 2011. Vertical distribution of larval fish in pelagic waters of southwest Lake Michigan: Implications for growth, survival, and dispersal. J. Gt. Lakes Res. **37**: 279-288. doi:10.1016/j.jglr.2011.01.006.

Milborrow, S. 2019. Plot 'rpart' Models: An Enhanced Version of 'plot.rpart. R package version 3.0.7. http://www.milbo.org/rpart-plot.

Miller, T.J., Crowder, L.B., Rice, I.A., and Marschall, E.A. 1988. Larval size and recruitment mechanisms in fishes: toward a conceptual framework. Can. J. Fish. Aquat. Sci. **45**: 1657-1670. doi:10.1139/f88-197.

Molony, B.W., and Choat, J.H. 1990. Otolith increment widths and somatic growth rate: the presence of a time-lag. J. Fish Biol. **37**: 541-551. doi:10.1111/j.1095-8649.1990.tb05887.x.

Mortimer, C.H. 2006. Inertial oscillations and related internal beat pulsations and surges in Lakes Michigan and Ontario. Limnol. Oceanogr. **51**(5): 1941-1955. doi:10.4319/lo.2006.51.5.1941.

Nalepa, T.F., Fanslow, D.L., Land, G.A. 2009. Transformation of the offshore benthic community in Lake Michigan: recent shift form the native amphipod *Diporeia* spp. To the invasive mussel *Dreissena rostriformis bugensis*. Freshw. Biol. **54**: 466-479.

Norden, C.R. 1968. Morphology and food habits of the larval alewife, Alosa pseudoharengus (Wilson), in Lake Michigan. Trans. Am. Fish. Soc. **96**(4): 387-393. doi:10.1577/1548-8659(1967)96[387:AGAFOT]2.0.CO;2.

O'Gorman, R., Lantry, B.F., and Schneider, C.P. 2004. Effect of stock size, climate, predation, and trophic status on recruitment of alewives in Lake Ontario, 1978–2000. Trans. Am. Fish. Soc. **133**(4): 855–867. doi:10.1577/ T03-016.1.

Okubo, A. 1971. Oceanic diffusion diagrams. Deep-Sea Res. Oceanogr. Abstr. **18**(8): 789-802. doi:10.1016/0011-7471(71)90046-5.

Pepin, P., Dower, J.F., and Benoît, H.P. 2001. The role of measurement error on the interpretation of otolith increment width in the study of growth in larval fish. Can. J. Fish. Aquat. Sci. **58**(11): 2204-2212. doi:10.1139/cjfas-58-11-2204.

Poje, A.C., Özgökmen, T.M., Lipphardt, B.L., Haus, B.K., Ryan, E.H., Haza, A.C., Jacobs, G.A., Reniers, A.J.H.M., Olascoaga, M.J., Novelli, G., Griffa, A., Beron-Vera, F.J., Chen, S.S., Coelho, E., Hogan, P.J., Kirwan, A.D., Huntley, H.S., and Mariano, A.J. 2014.

Submesoscale dispersion in the vicinity of the Deepwater Horizon spill. Proc. Natl. Acad. Sci. **111**(35): 12693-12698. doi:10.1073/pnas.1402452111.

Pothoven, S.A. and Fahnenstiel, G.L. 2015. Spatial and temporal trends in zooplankton assemblages along a nearshore to offshore transect in southeastern Lake Michigan from 2007 to 2012. J. Gt. Lakes Res. **41**(3): 95-103. doi:0.1016/j.jglr.2014.09.015.

Pritt, J.J., Roseman, E.F., O'Brien, T.P. 2014. Mechanisms driving recruitment variability in fish: comparisons between the Laurentian Great Lakes and marine systems. ICES J. Mar. Sci. **71**(8): 2252-2267. doi:10.1093/icesjms/fsu080.

R Core Team. 2013. R: A language and environment for statistical computing. R Foundation for Statistical Computing, Vienna, Austria. URL http://www.R-project.org/.

Rao, Y.R., and Murthy, C.R. 2001. Nearshore currents and turbulent exchange processes during upwelling and downwelling events in Lake Ontario. J. Geophys. Res. Oceans. **106**: 2667-2678. doi:10.1029/2000JC900149.

Rao, Y.R. and Schwab, D.J. 2007. Transport and mixing between the coastal and offshore waters in the great lakes: a review. J. Great Lakes Res. **33**(1): 202-218. doi:10.3394/0380-1330(2007)33[202:TAMBTC]2.0.CO;2.

Riley, S.C., Roseman, E.F., Nichols, S.J., O 'Brien, T.P., Kiley, C.S., and Schaeffer, J.S. 2008. Deepwater demersal fish community collapse in Lake Huron. Trans. Am. Fish. Soc. **137**: 1879–1890. doi:10.1577/T07-141.1.

Robert, D., Castonguay, M., and Fortier, L. 2007. Early growth and recruitment in Atlantic mackerel *Scomber scombrus*: discriminating the effects of fast growth and selection for fast growth. Mar. Ecol. Prog. Ser. **337**: 209-219. doi:10.3354/meps337209.

Rowe, M.D., Anderson, E.J., Wang, J., and Vanderploeg, H.A. 2015. Modeling the effect of invasive quagga mussels on the spring phytoplankton bloom in Lake Michigan. J. Gt. Lakes Res. **41**: 49-65. doi:10.1016/j.jglr.2014.12.018.

Rowe, M.D., Obenour, D.R., Nalepa, T.F., Vanderploeg, H.A., Yousef, F., and Kerfoot, W.C. 2015b. Mapping the spatial distribution of the biomass and filter-feeding effect of invasive dreissenid mussels on the winter-spring phytoplankton bloom in Lake Michigan. Freshw. Biol. **60**: 2270-2285. doi:10.1111/fwb.12653.

Rowe, M.D., Anderson, E.J., Wynne, T.T., Stumpf, R.P., Fanslow, D.L., Kijanka, K., Vanderploeg, H.A., Strickler, J.R., and Davis, T.W. 2016. Vertical distribution of buoyant Microcystis blooms in a Lagrangian particle tracking model for short-term forecasts in Lake Erie**.** J. Geophys. Res. Oceans. **121**: 5296-5314. doi:10.1002/2016JC011720.

Rowe, M.D., Anderson, E.J., Vanderploeg, H.A., Pothoven, S.A., Elgin, A.K., Wang, J.W., and Yousef, F. 2017. Influence of invasive quagga mussels, phosphorous loads, and climate

on spatial and temporal patterns of productivity in Lake Michigan: A biophysical modeling study. Limnol. Oceanogr. **62**(6): 2629-2649. doi:10.1002/lno.10595.

Schelske, C.L., Stoermer, E.F., Kenney, W.F. 2006. Historic low-level phosphorous enrichment in the Great Lakes interred form biogenic silica accumulation in sediments. Limnol. Oceanogr. **51**: 728-748. doi:10.4319/lo.2006.51.1_part_2.0728.

Schismenou, E., Palmer, M., Giannoulaki, M., Alvarez, I., Tsiaras, K., Triantafyllou, G., and Somarakis, S. 2016. Seasonal changes in otolith increment width trajectories and the effect of temperature of the daily growth rate of young sardines. Fish. Oceanogra. **25**(4): 362-372. doi: 10.1111/fog.12158.

Secor, D.H., and Dean, J.M. 1992. Comparison of otolith-based back-calculation methods to determine individual growth histories of larval striped bass, Morone saxatilis. Can. J. Fish. Aquat. Sci. **49**(7): 1439-1454. doi:10.1139/f92-159.

Thupaki, P., Phanikumar, M.S., and Whitman, R.L. 2013. Solute dispersion in the coastal boundary layer of southern Lake Michigan. J. Geophys. Res. Oceans. **118**: 1606-1617. doi: 10.1002/jgrc.20136.

Tsehaye, I., Jones, M.L., Bence, J.R., Brenden, T.O., Madenjian, C.P., and Warner, D.M. 2014. A multispecies statistical age-structured model to assess predator-prey balance: application to an intensively managed Lake Michigan pelagic fish community. Can. J. Fish. Aquat. Sci. **71**(4): 627-644. doi:10.1139/cjfas-2013-0313.

Vanderploeg, H.A., Pothoven, S.A., Fahnenstiel G.L., Cavaletto, J.F, Liebig, J.R., Stow, C.A., Nalepa, T.F., Madenjian, C.P., and Bunnell, D.B. 2012. Seasonal zooplankton dynamics in Lake Michigan: Disentangling impacts of resource limitation, ecosystem engineering, and predation during a critical ecosystem transition. J. Great Lakes Res. **38**: 336-352. doi:10.1016/j.jglr.2012.02.005.

Vikebø, F., Jørgensen, C., Kristiansen, T., and Fiksen, Ø. 2007. Drift, growth, and survival of larval Northeast Arctic cod with simple rules of behavior. Mar. Eco. Prog. Ser. **347**: 207-220. doi: 10.3354/meps06979.

Weber, M.J., Ruebush, B.C., Creque, S.M., Redman, R.A., Czesny, S.J., Wahl, D.H., and Dettmers, J.M. 2015. Early life history of alewife *Alosa pseudoharengus* in southwestern Lake Michigan. J. Gt. Lakes Res. **41**(2): 436-447. doi:10.1016/j.jglr.2015.03.009.

Withers, J.L., Sesterhenn, T.M., Foley, C.J., Troy, C.D., Höök, T.O. 2015. Diets and growth potential of early stage larval yellow perch and alewife in a nearshore region of southeastern Lake Michigan. J. Gt. Lakes Res. **3**: 197-209. doi:10.1016/j/jglr.2015.08.003.